Article

Ovule Transcriptome Analysis Discloses Deregulation of Genes and Pathways in Sexual and Apomictic *Limonium* Species (Plumbaginaceae)

Ana D. Caperta [1],*,† [ID], **Isabel Fernandes** [2],† [ID], **Sofia I. R. Conceição** [1,3] [ID], **Isabel Marques** [1,4] [ID], **Ana S. Róis** [1,5] [ID] and **Octávio S. Paulo** [2],* [ID]

1   Linking Landscape, Environment, Agriculture and Food (LEAF), Research Center, Associate Laboratory TERRA, Instituto Superior de Agronomia (ISA), Universidade de Lisboa, Tapada da Ajuda, 1349-017 Lisboa, Portugal; sconceicao@lasige.di.fc.ul.pt (S.I.R.C.); isabelmarques@isa.ulisboa.pt (I.M.); rois.ana@gmail.com (A.S.R.)
2   cE3c—Centre for Ecology, Evolution and Environmental Changes, CHANGE—Global Change and Sustainability Institute, Faculdade de Ciências, Universidade de Lisboa, 1749-016 Lisboa, Portugal; isabelcmoniz@gmail.com
3   LASIGE Computer Science and Engineering Research Centre, Faculdade de Ciências, Universidade de Lisboa, 1749-016 Lisboa, Portugal
4   Forest Research Centre (CEF), Associate Laboratory TERRA, Instituto Superior de Agronomia (ISA), Universidade de Lisboa, Tapada da Ajuda, 1349-017 Lisboa, Portugal
5   School of Psychology and Life Sciences, Universidade Lusófona de Humanidades e Tecnologias (ULHT), Campo Grande 376, 1749-024 Lisboa, Portugal
*   Correspondence: anadelaunay@isa.ulisboa.pt (A.D.C.); octavio.paulo@fc.ul.pt (O.S.P.)
†   These authors contributed equally to the work.

Abstract: The genus *Limonium* Mill. (sea lavenders) includes species with sexual and apomixis reproductive strategies, although the genes involved in these processes are unknown. To explore the mechanisms beyond these reproduction modes, transcriptome profiling of sexual, male sterile, and facultative apomictic species was carried out using ovules from different developmental stages. In total, 15,166 unigenes were found to be differentially expressed with apomictic vs. sexual reproduction, of which 4275 were uniquely annotated using an *Arabidopsis thaliana* database, with different regulations according to each stage and/or species compared. Gene ontology (GO) enrichment analysis indicated that genes related to tubulin, actin, the ubiquitin degradation process, reactive oxygen species scavenging, hormone signaling such as the ethylene signaling pathway and gibberellic acid-dependent signal, and transcription factors were found among differentially expressed genes (DEGs) between apomictic and sexual plants. We found that 24% of uniquely annotated DEGs were likely to be implicated in flower development, male sterility, pollen formation, pollen-stigma interactions, and pollen tube formation. The present study identifies candidate genes that are highly associated with distinct reproductive modes and sheds light on the molecular mechanisms of apomixis expression in *Limonium* sp.

Keywords: apomixis; floral development; functional annotation; Illumina sequencing; MADS-box; male sterility; sea lavenders; sexual reproduction; transcription factors

1. Introduction

Apomixis (agamospermy), the asexual seed production found in less than 1% of angiosperms [1], can be either independent of or dependent on pollination [2,3]. Most natural apomicts produce meiotic-reduced pollen involved in the fertilization of the polar nuclei in the embryo sac (pseudogamy) [2,3], but others reproduce independently of pollination for the initiation of the embryo or endosperm formation (autonomous apomicts) [4,5].

Different from sexual reproduction, apomixis is characterized by alterations in the developmental program during the formation and development of the female germline [2,6].

Apomicts can reproduce via gametophytic apomixis, involving the formation of an unreduced embryo sac (apomeiosis) that gives rise to a parthenogenetic embryo and a functional endosperm without the 2 maternal: 1 parental genome ratio [2,6]. The unreduced gametophytes can develop via restitutional meiosis or mitotic division (diplospory) or by a somatic, unreduced cell of the nucellus, which develops into an embryonic sac (apospory) [2,6]. In sporophytic apomicts (adventitious embryonies), the embryos originate from somatic tissues of the nucellus and/or integument cells. The formation of these apomictic embryos usually occurs in parallel with the formation of sexual embryos [7].

In gametophytic apomicts, pseudogamy is prevalent among aposporous apomicts, whereas autonomous endosperm formation seems to be prevalent in diplosporous apomicts [2,8]. These latter apomicts seem to be tolerant of deviations from a 2 maternal: 1 paternal genome contribution in the endosperm [4,5]. Autonomous apomicts tend to produce pollen with low viability and can even be male-sterile [9–13]. These apomicts include species from Asteraceae (e.g., *Crepis*, *Taraxacum* [9–11]), Plumbaginaceae (*Limonium* [12,13], Melastomataceae (*Miconia* [14], Poaceae (*Calamagrostis* [15]), and Rosaceae (*Alchemilla* [16]) genera, among others.

The emergence of apomixis in natural systems has been a long-standing topic of debate. It was hypothesized that the different types of apomixis are caused by different mutations that destabilize meiosis (megasporogenesis), the gametophyte (embryo sac), and egg formation [2,6]. Loci genetically linked to components of apomixis have been identified in various species, and sequencing of these loci has revealed several genes with the potential to play critical roles in apomixis [17,18]. It was hypothesized that apomixis could be caused by asynchronously expressed germline genes in the ovules of certain hybrids [19]. Transcriptome comparisons show that the genetic control of apomixis in gametophytic apomicts has been related to a wide range of mechanisms regulating gene expression, including protein degradation, transcription, cell cycle control, stress response, hormonal pathways, cell-to-cell signaling, and epigenetic mechanisms [18,20,21]. Several common genes found to be differentially expressed in multiple stages of apomictic and sexual seed production support the view that sexual and apomictic reproduction are closely related developmental pathways [22]. Recent studies present substantial evidence in support of a polyphenic condition for meiosis and determine that polyphenic shifts from apomeiosis to meiosis and vice versa are regulated by metabolic states [23].

The genus *Limonium* is a remarkable case study that could help with the identification of genetic-molecular factors potentially underlying apomixis [24]. The genus comprises c. 350 species with sexual and apomixis reproductive modes [25], having triploid and tetraploid apomicts with very large distributions in the Mediterranean region and the Atlantic coast [26–28]. The mode of speciation in the genus has been hypothesized to combine a polymorphic sexual system, hybridization under alloploid conditions, polyploidy combining autoploidy (unreduced pollen), allopolyploidy, and apomixis [13,24,25,29–31]. The polymorphic sexual system is associated with flower polymorphisms (ancillary pollen and stigma and/or heterostyly) and self-incompatibility (SI) under sporophytic control [29,30]. Coarsely reticulate pollen grains germinate on papillose stigmas and finely reticulate pollen grains germinate on cob-like stigmas, while the reverse combinations result in unsuccessful fertilization. Dimorphic SI species have two pollen stigma combinations and reproduce sexually as in diploids (*Limonium ovalifolium*, $2n = 16$ chromosomes). Monomorphic self-compatible species present self-fertile combinations, while monomorphic SI species show only one pollen-stigma combination and produce seeds through apomixis as in tetraploids (*Limonium multiflorum*; *Limonium dodartii*, $2n = 35, 36$) [12,28]. Sexual species form meiotically reduced tetrasporic embryo sacs [32–34] as in *L. ovalifolium* [13]. Whereas triploid and tetraploid facultative apomicts originate both reduced and unreduced, diplosporic apomictic embryo sacs (*Limonium oleifolium* (syn. *Statice oleaefolia*) [33]; *Limonium transwallianum* [34]. Pollen in *Limonium* apomitics ranges from low to high fertility or is not produced at all [12,25,31,35]. In the agamospermous species of the *L. binervosum* group (e.g., *Limonium binervosum s.s.*, *L. dodartii*, and *L. multiflorum*), male sterility, i.e.,

lack of viable pollen, is widespread, and male sterile colonies are confined to defined taxa/areas [12,13,26,28,36]. Male-sterile *L. multiflorum* plants from diverse colonies present aborted pollen with collapsed morphology without the typical exine patterns, pointing to a sporophytic defect [12]. The elevated number of seeds with high viability formed by this species seem to be the result of autonomous apomixis [13].

In this study, we aim to characterize the genetic factors implicated in *Limonium* reproductive modes by identifying the genes that are differentially expressed in ovules during sexual and apomixis seed production. Ovules in different stages of development were extracted to compare sexual (*Limonium auriculifolium* (syn. *Limonium nydeggeri* [37]), *L. ovalifolium*), putative facultative apomictic (*L. dodartii*), and male-sterile (*L. multiflorum*) plants, previously characterized cytogenetically, cytometrically, genetically, and reproductively [12,13,24,31] and used for profiling through RNA sequencing (RNA-Seq). This technology allows the identification of DEGs and the inference of their expression with high accuracy [38]. Downstream analysis, including functional annotation of the assembled transcriptome and GO enrichment analysis of the annotated DEGs, was used to provide meaningful biological insights that contribute to a better understanding of the molecular mechanisms and pathways that control the switch from sexual reproduction to apomixis in the organisms under study. Our experimental approach was designed to overcome difficulties due to the occurrence of differing patterns among reproductive modes. The specific goals of this study were to: (1) identify transcripts showing differential expression between male-sterile *L. multiflorum* and sexual plants; (2) partition DEGs into groups whose fold-changes reflect genes potentially involved in flower development; and (3) frame our findings according to previous and ongoing studies to understand apomixis regulation in *Limonium*.

2. Materials and Methods

2.1. Plant Material

Plants from four *Limonium* species were selected to represent different reproductive modes, i.e., diploid sexual as *L. auriculifolium* ($n = 2$) and *L. ovalifolium* ($n = 2$; $2n = 2x = 16$ chromosomes) [12,13], tetraploid apomictic as *L. multiflorum* ($n = 2$; $2n = 4x = 35$), and the facultative apomictic *L. dodartii* ($n = 1$; $2n = 4x = 35$) [13,24]. These plants, grown from seedlings raised from seed collected in the wild, were maintained at the ex situ collection in a semi-closed greenhouse at the Instituto Superior de Agronomia, Lisbon (Table 1).

Table 1. List of all tested and control samples of *Limonium* compared in the differential expression analysis, according to species, reproductive strategy, stage (S), and number of replicates (Rep). Number of all and annotated significantly differentially expressed genes (DEGs) detected by edgeR in *Limonium* plants, namely apomictic *L. multiflorum* (M), sexual *L. auriculifolium* (A/a) and *L. ovalifolium* (O/o), and facultative apomictic *L. dodartii* (d), in either stage S1 (1), S2 (2), or S3/S4 (4). All DEGs represent the number of significant genes found to be differently expressed between each test and control sample. DEG annotation was performed according to *A. thaliana* reference genome. [Comparisons: uppercase refers to test samples, lowercase refers to control samples, and numbers refer to respective stages].

Test Samples (T)		Control Samples (c)		Comparison	All DEGs	Annotated DEGs		
Species	Stage (Rep)	Species	Stage (Rep)			Total	Up (%)	Down (%)
				Apomictic vs. sexual				
L. multiflorum (M) [Apomictic]	S1 (R1)	*L. auriculifolium* (a) [Sexual]	S1 (R1)	**M1a1**	3517	1080	453 (42%)	627 (58%)
			S2 (R1)	**M1a2**	2785	663	295 (44%)	368 (56%)
	S2 (R1-5)		S3/S4 (R1)	**M2a4**	4400	1174	489 (42%)	685 (58%)
	S1 (R1-4)	*L. ovalifolium* (o) [Sexual]	S1 (R1)	**M1o1**	3068	809	371 (46%)	438 (54%)
			S2 (R1)	**M1o2**	3054	1018	419 (41%)	599 (59%)
	S2 (R1-5)		S3/S4 (R1)	**M2o4**	12,839	3544	2827 (80%)	717 (20%)

Table 1. *Cont.*

Test Samples (T)		Control Samples (c)		Comparison	All DEGs	Annotated DEGs		
Species	Stage (Rep)	Species	Stage (Rep)			Total	Up (%)	Down (%)
				Apomictic vs. facultative apomictic				
	S2 (R1-5)	*L. dodartii* (d) [Facultative apomictic]	S4 (R1-3)	**M2d4**	806	226	41 (18%)	185 (82%)
				Between stages comparisons (same species)				
	S2 (R1-5)	*L. multiflorum* (M) [Apomictic]	S1 (R1-4)	**M2m1**	1096	387	379 (98%)	8 (2%)
L. auriculifolium (A) [Sexual]	S2 (R1)	*L. auriculifolium* (a) [Sexual]	S1 (R1)	**A2a1**	796	276	40 (14%)	236 (86%)
	S3/S4 (R1)			**A4a1**	351	111	93 (84%)	18 (16%)
			S2 (R1)	**A4a2**	1346	471	356 (76%)	115 (24%)
	S2 (R1)	*L. ovalifolium* (o) [Sexual]	S1 (R1)	**O2o1**	693	208	189 (91%)	19 (9%)
	S3/S4 (R1)			**O4o1**	2067	711	395 (56%)	316 (44%)
L. ovalifolium (O) [Sexual]			S2 (R1)	**O4o2**	1650	526	228 (43%)	298 (57%)
				Between species comparisons (sexual)				
	S1 (R1)	*L. auriculifolium* (a) [Sexual]	S1 (R1)	**O1a1**	616	200	34 (17%)	166 (83%)
	S2 (R1)		S2 (R1)	**O2a2**	1242	367	273 (74%)	94 (26%)
	S3/S4 (R1)		S3/S4 (R1)	**O4a4**	1611	550	257 (47%)	293 (53%)

2.2. Ovule Extraction

Flower buds at distinct developmental stages were sampled prior to anthesis according to their size (between 2 and 5 mm) based on cytoembryological observations as in [13], at standardized times (between 9:00 a.m. and 12:00 p.m.). The ovules were selected with respect to the timing of apomeiosis (Stage 1—S1), megagametogenesis (embryo sac, Stage 2—S2), parthenogenesis, and endosperm formation (Stages 3/4—S3/S4), detailed in [13]. Dissection of ovules was performed in a sterile laminar air flow cabinet under a stereoscopic microscope (Stemi 2000-C, Zeiss) with the aid of tweezers and pencil-point spinal needles (Transmed). In total, 280 ovules were extracted from each ovary, containing one ovule each, and about ten to twenty ovules per stage were isolated and placed in a sterile Petri dish with B5 medium [39] to maintain hydration before RNA extraction. This procedure generated a total of 18 samples, including nine samples of ovules from apomictic plants (four biological replicates in stage S1 and five biological replicates in stage S2) and three samples from each of the remaining species (sexual: two species x three stages—S1, S2, and S3/S4; facultative apomictic: three biological replicates in stage S3/S4) (Table 1).

2.3. Total RNA Extraction and Library Preparation

Total RNA was extracted from all samples using the Spectrum™ Plant Total RNA Kit (Sigma-Aldrich, St. Louis, MO, USA). Nevertheless, some modifications were required for obtaining high-quality RNA, as detailed. Samples were collected in 150 µL of lysis solution and grounded with the help of a micropestle in the microfuge tube. Then, another 300 µL of lysis solution supplemented with β-mercaptoethanol was added to the tube, which was vortexed vigorously and incubated at 56 °C for 5 min. The lysate was centrifuged at 14,000 rpm for 2 min, and then the supernatant was transferred into a filter column and centrifuged for 1 min at 14,000 rpm. The clarified flow-through lysate was transferred to a new tube, and 250 µL of Binding Solution was added. The mixture was applied to a binding column and centrifuged for 1 min at 14,000 rpm. The remaining steps followed the manufacturer's instructions. The quantity of RNA was determined using a BioDrop cuvette (BioDrop, Cambridge, UK) and electrophoresis on a 1% agarose gel. The RNA integrity number (RIN) was determined using an Agilent 2100 Bioanalyzer (Agilent Technologies, Santa Clara, CA, USA) and ranged from 9.19 to 9.45. The messenger RNA (mRNA) libraries were constructed with the Illumina "TruSeq Stranded mRNA Sample Preparation kit" (Illumina, San Diego, CA, USA) and sequenced on an Illumina NovaSeq6000 2× 100 bp at Macrogen facilities (Macrogen, Geumcheon-gu, Seoul, Korea).

2.4. Processing, Mapping, and Quantification of Illumina Reads

All raw reads have been deposited in the NCBI Sequence Read Archive (SRA), Bio-Project accession PRJNA752506. Quality control of the raw reads, including contaminants survey, was performed using FastQC version 0.11.9 [40] and FastQ Screen version 0.14.0 [41], which ran against the genomes of their default pre-indexed species and adaptors. Then, since all raw reads presented a quality base score over 36, Trimmomatic version 0.39 [42] was used to eliminate adaptors and filter reads of length below 36 base pairs (bp). A de novo transcriptome assembly was performed using Trinity version 2.11.0 [43], in which cleaned reads from all samples were combined to generate one global assembly since this software has shown consistent performance and has a high read alignment rate [44]. The assembly was assessed for completeness using BUSCO version 5 [45] through gVolante2 [46]. After alignment against the transcriptome using Bowtie2 aligner version 2.3.5 [47], sequences were quantified at gene-level expression with RSEM version 1.3.3 [48] through the Trinity pipeline. A principal component analysis (PCA) was performed to survey the relatedness of normalized gene counts using the function plotPCA in R Studio version 4.0.2 [49].

2.5. Differentially Expressed Genes Detection

To study significant differences between apomictic and sexual plants, differential expression analysis was performed with edgeR version 3.30.3 [50], which is a flexible empirical Bayes approach that uses weighted likelihood methods to estimate gene-specific variation even with very few or no replicates [51]. Overall, when studying differences between reproductive strategies, apomictic plants were set as the samples to test, while sexual and facultative apomictic plants were set as the controls, according to each comparison (Table 1). As such, up-regulated DEGs are more expressed in apomictic than in sexual plants, while down-regulated DEGs are less expressed in apomictic and more expressed in sexual plants.

Genes with a normalized $|\log2$ fold change (log2 FC)$| > 2$ were defined as differentially expressed and used in the downstream analysis. In the comparison between apomictic and facultative apomictic plants, in which all samples have at least 3 replicates, DEGs were previously filtered by $p < 0.01$. Venn diagrams were used to plot DEGs between different comparisons through matplotlib version 3.3.3 [52] in Python version 3.9.0 (Python Software Foundation 2020). Additionally, DEGs commonly triggered by more than one comparison were searched for opposite regulation.

2.6. Functional Annotation

Functional annotation of DEGs was performed with the Basic Local Alignment Search Tool (BLAST) version 2.10.1 command-line tool from the NCBI C++ Toolkit (National Center for Biotechnology Information 2020). Blastx was used to map DEGs to *A. thaliana* homologs against a local Swissprot database, filtering gene hits by a maximum E-value of $1.0E^{-3}$ and a minimum identity of 40%. [53]. Then, to avoid duplicated results, DEGs annotated to the same *A. thaliana* homolog were filtered by identities and sequence length, keeping the transcripts with the highest values.

Housekeeping genes (HKGs) are typically required for the maintenance of basal cellular functions that are essential for its existence, regardless of their specific role in the tissue or organism. Since these genes are usually highly conserved, genes stably transcribed in all comparisons were filtered. Additionally, DEGs were searched for the most common housekeeping homolog genes in *A. thaliana* to study their potential role in reproduction in *Limonium* plants.

In addition, DEGs were searched for sRNA biogenesis, which is known to play pivotal roles in reproductive development [54,55], and oxidative stress-related genes, which negatively affect reproductive development in plants [56]. DEGs associated with tryptophan and ethylene metabolism were investigated, which are associated with the biosynthesis and regulation of the phytohormone auxin, a vital component of plant reproduction since it regulates both male and female reproductive organs [57,58]. Moreover, DEGs

related to aminoacyl-tRNA metabolism and lysine degradation, which are respectively essential to produce ribosomes and proteins, and epigenetic processes through DNA methylation [59,60] were searched.

2.7. Transcription Factors (TFs) Involved in Plant Reproduction

TFs can be engaged in plant reproduction, namely in flower development such as *APETALA* (AP genes: *AP1*, *AP2*, and *AP3*), *PISTILLATA* (*PI*), *SEPALLATA* (SEP genes: *SEP1*, *SEP3*), and other MADS-box TFs [61–63], and in male sterility (e.g., *ROS1*, *DMC1*, *MS2*, *POP1*, and *4CLL1*; [64,65]. As such, these genes, along with a list of *A. thaliana* TFs retrieved from the Plant Transcription Factor and Protein Kinase Identifier and Classifier database (iTAK v18.12) [66], were searched among DEGs to find if they were down-regulated in apomictic plants. Next, KEGG and WikiPathways enrichment analysis was performed with gProfiler to find relevant metabolic pathways among these TFs, following the same parameters mentioned for GO analysis (see below). Furthermore, uniquely annotated lists of DEGs were searched for GO terms related to pollen, such as the direct and child terms of the biological processes "microsporocyte differentiation" (GO:0010480), "pollen development" (GO:0009555), "pollen wall" (GO:0043667), "pollen coat" (GO:0070505), "pollination" (GO:0009856), and the "cellular components pollen tube" (GO:0090406), according to UniProtKB and StringDB.

2.8. Enrichment Analysis

Uniquely annotated DEGs were characterized with GO terms using the REST API on the UniprotKB website (The Uniprot Consortium, 2019). Finally, GO enrichment analyses were applied to log2FC-ordered lists of DEGs through an over-representation analysis (ORA) using the g:GOSt functional profiling tool from the gProfiler website [67], with the g:SCS tailored algorithm under FDR < 0.01, using a predefined *A. thaliana* custom background including only genes expressed by the samples in analysis. Enrichment results were summarized using REVIGO [68] through the removal of redundant GO terms with allowed similarity = 0.5 and then plotted with the R ggplot2 version 3.3.2 library [69]. To better understand the differences between the initial and final stages of both sexual and apomictic plants, ORA results were filtered by specificity to a particular stage.

3. Results

3.1. Gene Expression

The assembled transcriptome generated a total of 162520 trinity unigenes with a 43% GC content and a contig N50 of 2128 (Supplementary Table S1) According to BUSCO, 90% completeness was achieved in the de novo assembled transcriptome, indicating that we have generated a high-quality transcriptome assembly that could be used for further downstream analysis (Supplementary Table S1). The total number of expressed unigenes among *Limonium* samples was highest in ovules from *L. multiflorum* (apomictic) in stage S2 (115775), followed by *L. dodartii* (facultative apomictic) in stage S4 (103345), and varying from 20133 to 76395 in sexual plants (Table 2). Among these, the number of expressed unigenes in *L. auriculifolium* was higher than that in *L. ovalifolium* in stages S3/S4, but lower in the remaining stages (Table 2). In the PCA, PC1, which accounted for 71% of the variance, revealed a clear cluster of sexual plants on the right side of the graph (Supplementary Figure S1). The PC2 separated sexual ovules in the S1 and S2 stages (upper-right quadrant) from sexual ovules in the S3/S4 stage (lower-right quadrant). Moreover, PC1 grouped all samples from apomictic and facultative apomictic plants with ovules in stage S1 (Supplementary Figure S1, left), showing a higher dispersion in the remaining stages of these ovules.

Table 2. Total number of genes expressed by *Limonium* samples from apomictic *L. multiflorum* (M), facultative apomictic *Limonium dodartii* (d), and sexual *L. auriculifolium* (A/a) and *L. ovalifolium* (O/o) ovules in stages S1, S2, and S3/S4.

Reproduction	Species	Stages		
		S1	**S2**	**S3/S4**
Apomictic	*L. multiflorum* (M)	933936	115775	-
Facultative apomictic	*L. dodartii* (d)	-	-	103,345
Sexual	*L. auriculifolium* (A/a)	60,143	48,851	61,550
	L. ovalifolium (O/o)	67,207	76,395	20,133

Several HKGs were found in all comparisons of *Limonium* plants, regardless of species, reproductive strategy or stage, namely: ACT domain-containing proteins (*ACR3, ACR8,* and *ACR9*), actin (*ACT2, ACT4,* and *ACT7*), actin-depolymerizing factors (*ADF1* and *ADF10*), actin-interacting proteins (*AIP1-1, AIP1-2*), actin-related proteins (*ARP2, ARP6,* and *ARP8*), cytosolic Fe-S cluster assembly factor *NBP35*, expansins (*EXPA2* and *EXPA9*), glyceraldehyde-3-phosphate dehydrogenase *GAPA1*, heat shock proteins (*HSP90-4* and *HSP90-5*), NADH dehydrogenase [ubiquinone] flavoprotein 2 (*NDUFV2*), phosphoglycerate kinase 1 (*PGK1*), polyubiquitin 3 (*UBQ3*), TATA-box-binding protein 2 (*TBP2*), tubby-related proteins (*TULP1* and *TULP3*) and tubulins (*TUB1, TUBB1, TUBB4,* and *TUBB7*).

3.2. Overall Differential Expression Analysis

The highest number of annotated DEGs (3544) was found in M2o4, followed by M2a4 (1174) (Table 1). In intraspecies comparisons, *L. ovalifolium* showed the lowest number of DEGs in O2o1 (693), followed by O4o2 (1650), with the major differences being observed in O4o1 (2067; Supplementary Figures S2B and S3C,D). Conversely, *L. auriculifolium* showed the lowest differences in A4a1 (351), followed by A2A1 (796), thus presenting the major differences in A4a2 (1346; Supplementary Figures S2A and S3A,B). Notably, DEGs showed a proportion of 24% to 35% unannotated genes across samples (Table 1). On the other hand, M1o1 and M1o2 showed just slightly more DEGs than M1a2, while M2m1 presented more DEGs than M2d4. When comparing the two sexual plants, there was an increasing number of DEGs with the progression of stages, which varied from 616 to 1611 (Table 1; Supplementary Figure S2C).

When comparing DEGs between apomictic and sexual species, among sexual plants in S1, 47% (602) were found both in M1a1 and M1o1, while in S2, 32% (407) were found both in M1a2 and M1o2 (Figure 1A,B). The number of specific DEGs was higher in M1a1 than in M1o1 (478 vs. 207), but lower in M1a2 than in M1o2 (256 vs. 611). Moreover, the number of specific DEGs was much higher in M2o4 than in M2a4 (2562 vs. 272), with the lowest in M2d4 (71; Figure 1C).

Some DEGs were detected in more than one developmental phase, although they presented opposite regulations (Supplementary Table S2; Supplementary Figure S4). Only four DEGs were down-regulated in M1a1 and up-regulated in M1o1, including FPF1, associated with flower development. Furthermore, 124 DEGs were down-regulated in M2a4, including *ABCG28, ADPG2, AGL66, ATXR5, CALS5, CNGC18, LRL1, PRK3, PS1, SHT, TIP5-1, WRKY2* associated to anther and pollen development, but up-regulated in M2o4, while 5 DEGs presented the opposite regulation, namely *SEU*, which is involved in flower development. Additionally, 11 DEG were up-regulated in M2a4 but down-regulated in M2d4, being mainly linked to stress responses. Moreover, 44 DEGs were up-regulated in M2o4 but down-regulated in M2d4, which included QRT2, related to anther and pollen.
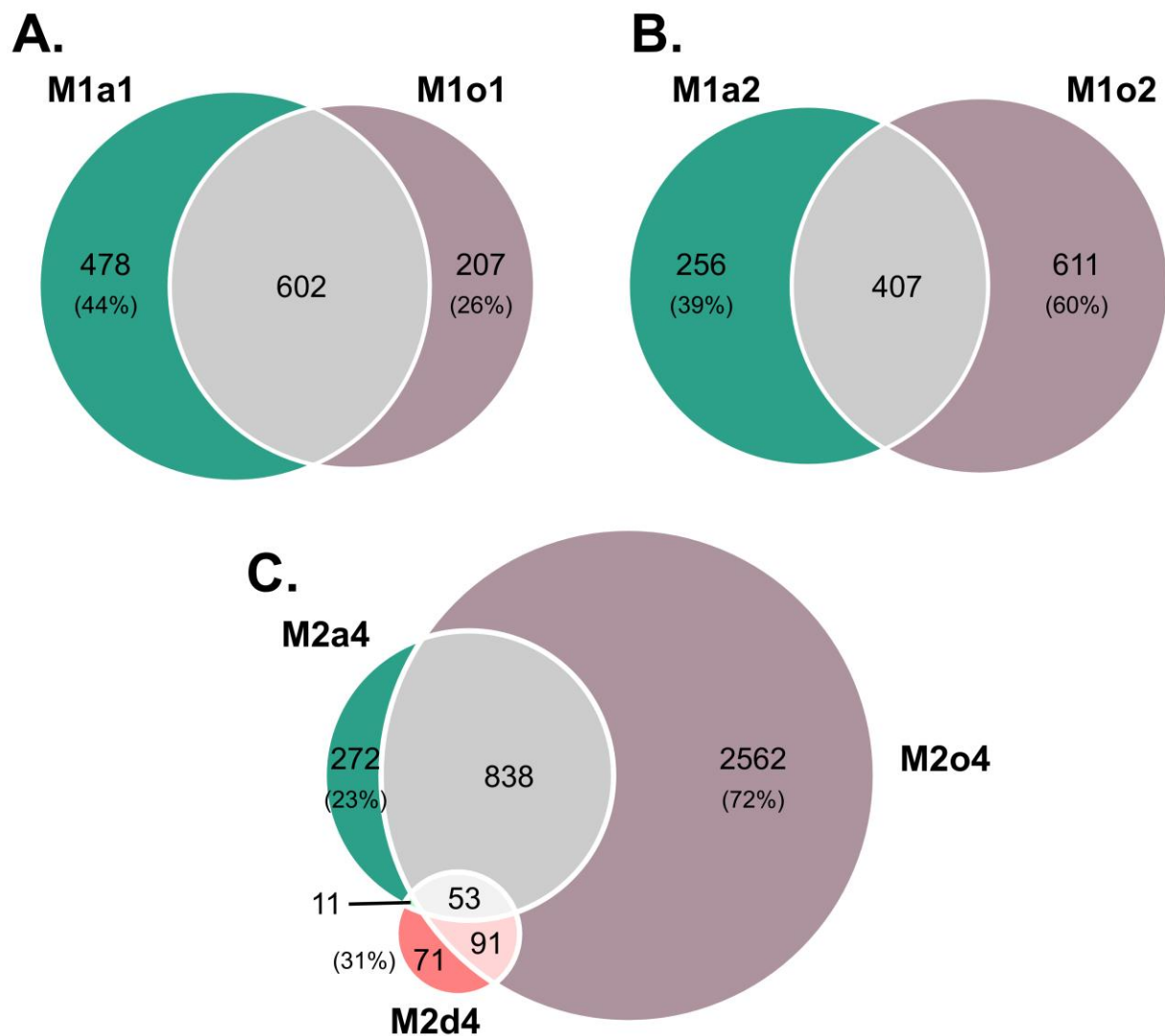
Figure 1. Weighted Venn diagrams of specific and overlapping differentially expressed genes (DEGs) found in the ovules of apomictic *L. multiflorum* (M), facultative apomictic *L. dodartii* (d), and sexual *L. auriculifolium* (a) and *L. ovalifolium* (o). DEGs were filtered by |log2 fold-change (log2FC)| > 2. Number of overlapping and specific DEGs in: A. *L. multiflorum* in S1 relative to *L. auriculifolium* in S1 (M1a1; green) and to *L. ovalifolium* in stage S1 (M1o1; purple); B. *L. multiflorum* in S1 relative to *L. auriculifolium* in S2 (M2a2; green) and to *L. ovalifolium* in S2 (M1o2; purple); C. *L. multiflorum* in S2 relative to *L. auriculifolium* in S3/S4 (M2a4; green), to *L. ovalifolium* (M2o4; purple) and to *L. dodartii* in S4 (M2d4; red).

3.3. DEGs Potentially Implicated in Apomixis Regulation

Some common HKGs in *A. thaliana* were found to be differentially expressed in apomictic *Limonium* plants, namely *A1*, *ACR11*, two *ACT*, seven *EXPA*, two *GAPC*, *HSP90-6*, *RALFL19*, four *TUBB*, and eight *UBC* genes. While *EXPA* and *TUBB* DEGs were mainly down-regulated in apomictic plants, the remaining genes were mostly up-regulated (Table 3).

Table 3. List of common housekeeping genes in *A. thaliana* (gene name) that were differentially expressed (DEGs) in the ovules of apomictic *L. multiflorum* (M) in S1 and S2, and sexual *L. auriculifolium* (a) and *L. ovalifolium* (o) in S1, S2, and S3/S4. DEGs were filtered by |log2 fold-change (log2FC)| >2 (red: up-regulated DEGs; blue: down-regulated DEGs).

Gene ID	Gene Name	Protein Name	Log2FC						
			M1a1	M1a2	M1o1	M1o2	M2a4	M2o4	M2d4
TRINITY_DN12562_c0_g1	*A1*	Elongation factor 1-α						10.09	
TRINITY_DN9323_c2_g1	*ACR11*	ACT domain-containing protein ACR11						7.81	
TRINITY_DN594_c3_g1	*ACT1*	Actin-1						7.09	
TRINITY_DN3478_c1_g1	*ACT11*	Actin-11					−4.39	−2.32	
TRINITY_DN13623_c0_g1	*EXPA11*	Expansin-A11					−5.35	−5.85	
TRINITY_DN2256_c1_g1	*EXPA13*	Expansin-A13	−2.28			−2.07	−2.17	−3.78	
TRINITY_DN27728_c0_g1	*EXPA15*	Expansin-A15						6,5	
TRINITY_DN151736_c0_g1	*EXPA16*	Expansin-A16					−4.77	−2.4	−2.06
TRINITY_DN12567_c0_g1	*EXPA20*	Expansin-A20					−2.08	7.23	
TRINITY_DN21891_c0_g1	*EXPA6*	Expansin-A6	−2.41			−2.42			
TRINITY_DN5240_c0_g1	*EXPA8*	Expansin-A8	−5.09	−3.65	−3.79	−4.76	−2.76	−3.16	
TRINITY_DN10654_c0_g1	*GAPC1*	Glyceraldehyde-3-phosphate dehydrogenase GAPC1, cytosolic		8.03	2.95				
TRINITY_DN10775_c0_g1	*GAPC2*	Glyceraldehyde-3-phosphate dehydrogenase GAPC2, cytosolic					−2.67	−2.02	
TRINITY_DN638_c0_g1	*HSP90-6*	Heat shock protein 90-6, mitochondrial						9.87	
TRINITY_DN28088_c0_g2	*RALFL19*	Probable ubiquitin-conjugating enzyme E2 24	−7.67	−4.99	−4.97	−7.43	−4.92	−4.37	
TRINITY_DN521_c0_g6	*TUBB5*	Tubulin β-5 chain					−2.46	−3.5	
TRINITY_DN159888_c0_g1	*TUBB6*	Tubulin β-6 chain	−2.58					−2.21	
TRINITY_DN2826_c0_g1	*TUBB8*	Tubulin β-8 chain						11.41	
TRINITY_DN2332_c0_g1	*TUBB9*	Tubulin β-9 chain						8.91	
TRINITY_DN6957_c0_g1	*UBC10*	Ubiquitin-conjugating enzyme E2 10						8.36	
TRINITY_DN193932_c0_g1	*UBC11*	Ubiquitin-conjugating enzyme E2 11						6.39	2.72
TRINITY_DN184540_c0_g1	*UBC19*	Ubiquitin-conjugating enzyme E2 19	−3.31		−3.22	−3.64			
TRINITY_DN6909_c0_g1	*UBC29*	Ubiquitin-conjugating enzyme E2 29	3.03		2.14	3.94	4.14	14.61	
TRINITY_DN2966_c0_g1	*UBC33*	Probable ubiquitin-conjugating enzyme E2 33	2.1				5.58	9.74	
TRINITY_DN43968_c0_g1	*UBC35*	Ubiquitin-conjugating enzyme E2 35					3.13	6.36	
TRINITY_DN10935_c1_g1	*UBC4*	Ubiquitin-conjugating enzyme E2 4						7.32	
TRINITY_DN10551_c0_g1	*UBC8*	Ubiquitin-conjugating enzyme E2 8	2.06	2.34				6.99	

Oxidative stress-related DEGs were found to be mainly up-regulated in apomictic plants, namely *ACO3*, *CDSP32*, *GSH1*, *GSTU20*, *ABC1K8*, and *APX6* (Supplementary Figure S2). However, *GR1*, *GASA14* (GASA—GA-stimulated transcripts), and *GSTF11*, which are also related to oxidative stress, were down-regulated. Some genes presented mixed regulation, with *GSTU19* being down-regulated in M1o2 but up-regulated in M1a2 and M2o4, and *MIOX* being up-regulated in all comparisons except M2d4, which was down-regulated (Supplementary Figure S5A).

Analyzing DEGs associated with sRNA biogenesis showed an up-regulation of various genes like *AGO1*, *AGO4*, *AGO5*, *AGO7*, *AGO8*, *AGO9*, *DML2*, and *DNMT2* in M2o4. Nevertheless, in the remaining comparisons between apomictic and sexual ovules, while there was a down-regulation of *AGO5* and *AGO10* in apomictic ovules, DML2 was up-regulated in the same plants (Supplementary Figure S5B).

3.4. Floral-Related DEGs

Globally, the most differentially expressed genes between apomictic and sexual ovules in the early stages were associated with floral development (Supplementary Tables S3 and S4). In M1a1, top-DEGs included a down-regulation of *AP3*, *PI*, and *PEX4* (log2FC: −8.66, −8.50, and −8.44), while *AP1* and *SEP1* were among the top down-regulated DEGs in M1a2 (log2FC: −7.24 and −7.09) (Supplementary Table S3). In M1o1, top down-regulated DEGs included *SEP1* and *GASA7* (log2FC: −7.56 and −7.43), while *AP3* was down-regulated in top-DEGs in M1o2 (log2FC: −8.55) (Supplementary Table S4). Overall, top-DEGs from

M2a4, M2o4, and M2d4 were implicated in general molecular functions, such as binding, a structural constituent of the ribosome, and catalytic, transporter, structural molecule, ATP-dependent, and transcription regulator activities, presenting a higher log2FC variation in M2a4 (-8.30 to 12.35) and M2o4 (-8.52 to 16.87) than in M2d4 (-5.91 to 8.57) (Supplementary Tables S3–S5). Moreover, among top-DEGs in M2m1, two genes presented opposite regulation, with *GASA1* being down-regulated and *AGL15* being up-regulated (log2FC: -4.61 to 8.81) (Supplementary Table S6). In the remaining comparisons, there was also a predominance of general molecular functions (Supplementary Tables S7–S9).

In the early stages, among all DEGs between apomictic and sexual ovules, there was a predominant down-regulation of *AP*, *PI*, and *SEP* in apomictic plants. Additionally, it was found that AGAMOUS (AG) genes (e.g., *AGL42*) were up-regulated, as were other MADS-box genes, namely *ANR1*, *FLC*, *SOC1*, and *SVP*. However, M2o4 showed both up- and down-regulation of AP genes. Other MADS-box genes were also both up- and down-regulated in M2a4 and M2o4 (Figure 2 and Table 4).
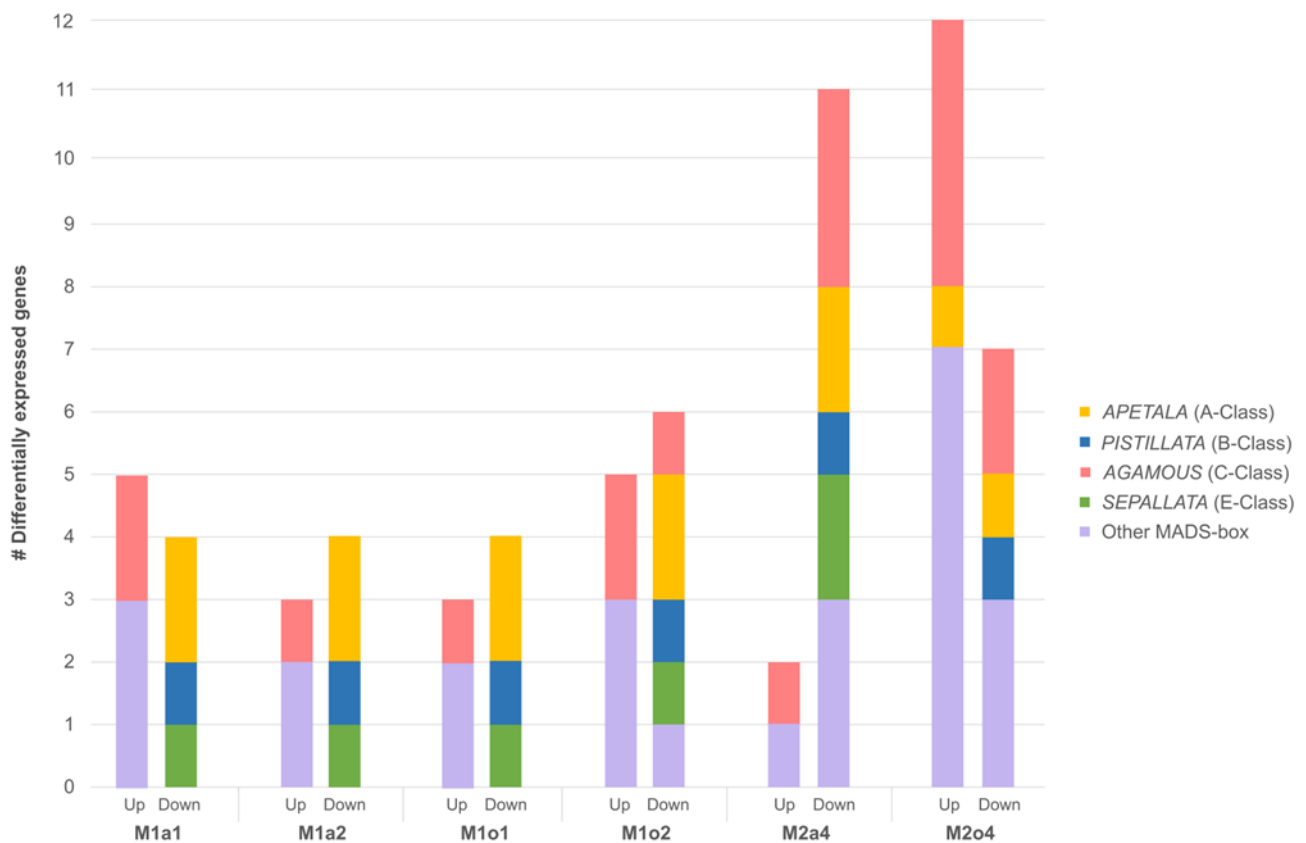
Figure 2. Distribution of differentially expressed genes related to floral development in ovules from apomictic *L. multiflorum* (M), sexual *L. auriculifolium* (a) and *L. ovalifolium* (o), and facultative apomictic *L. dodartii* (d). Differentially expressed MADS-box genes *APETALA* (A-class), *PISTILLATA* (B-class), *AGAMOUS* (C-class), *SEPALLATA* (E-class), and other MADS-box genes are represented. DEGs were found in apomictic ovules in S1 relative to sexual ovules in S1 (M1a1 and M1o1) and S2 (M1a2 and M1o2), and relative to sexual ovules in S3/S4 (M2a4 and M2o4), and facultative apomictic in S4 (M2d4).

Table 4. List of florally differentially expressed genes (DEGs) in ovules of *Limonium* plants, namely apomictic *L. multiflorum* (M), sexual *L. auriculifolium* (a), and *L. ovalifolium* (o). DEGs were found in apomictic ovules in S1 relative to sexual ovules in S1 (M1a1 and M1o1) and S2 (M1a2 and M1o2), and in apomictic ovules in S2 relative to sexual ovules in S3/S4 (M2a4 and M2o4); (red: up-regulated DEGs; blue: down-regulated DEGs).

| Gene ID	Gene Name	Protein Name	Log2FC					
			M1a1	M1a2	M1o1	M1o2	M2a4	M2o4
TRINITY_DN28291_c0_g2	AGL15	Agamous-like MADS-box protein AGL15					−4.08	7.12
TRINITY_DN13295_c0_g1	AGL16	Agamous-like MADS-box protein AGL16	2.14	2.21				9.13
TRINITY_DN610_c1_g1	AGL42	MADS-box protein AGL42				2.15		
TRINITY_DN2793_c0_g2	AGL6	Agamous-like MADS-box protein AGL6						7.9
TRINITY_DN3873_c0_g1	AGL65	Agamous-like MADS-box protein AGL65				−2.29	−2.62	−3.28
TRINITY_DN12180_c0_g1	AGL66	Agamous-like MADS-box protein AGL66					−4.72	−3.81
TRINITY_DN342_c0_g2	AGL8	Agamous-like MADS-box protein AGL8	4.02		2.86	4.34	2.59	6.91
TRINITY_DN72066_c0_g2	ANR1	MADS-box transcription factor ANR1						6.03
TRINITY_DN9027_c0_g3	AP1	Floral homeotic protein APETALA 1	−7.1	−7.24	−7.17	−6.32		
TRINITY_DN2754_c0_g1	AP2	Floral homeotic protein APETALA 2						2.14
TRINITY_DN7779_c0_g1	AP3	Floral homeotic protein APETALA 3	−8.66	−6.05	−6.98	−8.55	−4.17	−3.22
TRINITY_DN46144_c0_g1	ATH1	Homeobox protein ATH1		3				7.07
TRINITY_DN27333_c1_g1	BLH8	BEL1-like homeodomain protein 8						7.15
TRINITY_DN1609_c0_g1	BRI1	Protein BRASSINOSTEROID INSENSITIVE 1	−2.45			−2.2		
TRINITY_DN17115_c0_g1	CCA1	Protein CCA1						7.18
TRINITY_DN11983_c0_g1	CDF2	Cyclic dof factor 2						2.81
TRINITY_DN2531_c1_g2	COL5	Zinc finger protein CONSTANS-LIKE 5	2.15			2.71	2.27	
TRINITY_DN26110_c0_g1	CSTF77	Cleavage stimulation factor subunit 77						2.13
TRINITY_DN22923_c0_g1	ELF6	Probable lysine-specific demethylase ELF6						5.1
TRINITY_DN3347_c0_g1	EMF2	Polycomb group protein EMBRYONIC FLOWER 2						2.89
TRINITY_DN7896_c0_g2	FLC	MADS-box protein FLOWERING LOCUS C						8.63
TRINITY_DN5378_c0_g1	FPA	Flowering time control protein FPA						3.27
TRINITY_DN184585_c0_g1	FPF1	Flowering-promoting factor 1	2.72		2.94	3.9	2.94	3.58
TRINITY_DN7899_c0_g1	FT	Protein FLOWERING LOCUS T				2.06		2.37
TRINITY_DN344_c1_g2	GA2	Ent-kaur-16-ene synthase, chloroplastic			3.21			7.82
TRINITY_DN2317_c0_g2	GA2OX6	Gibberellin 2-β-dioxygenase 6	3.87			3.85	3.72	11.51
TRINITY_DN38605_c0_g1	GA2OX8	Gibberellin 2-β-dioxygenase 8						−4.06
TRINITY_DN13033_c0_g1	GA3OX1	Gibberellin 3-β-dioxygenase 1					2.87	8
TRINITY_DN8333_c0_g1	GA3OX2	Gibberellin 3-β-dioxygenase 2						11.4
TRINITY_DN17736_c0_g1	GASA1	Gibberellin-regulated protein 1	4.81	2.37	2.98	5.17		
TRINITY_DN10114_c0_g1	GASA11	Gibberellin-regulated protein 11	2.56	2.1	2.79	2.59		9.79
TRINITY_DN31284_c0_g1	GASA14	Gibberellin-regulated protein 14					−2.5	−4.11
TRINITY_DN185389_c0_g1	GASA3	Gibberellin-regulated protein 3					−5.19	−4.01
TRINITY_DN5658_c0_g1	GASA6	Gibberellin-regulated protein 6	−4.47	−2.13	−2.06	−4.55	−4.83	−5.73
TRINITY_DN1467_c0_g1	GASA7	Gibberellin-regulated protein 7	−7.76	−6.05	−7.43	−7.99	−4.99	−4.24
TRINITY_DN8938_c0_g1	GASA9	Gibberellin-regulated protein 9		−2.47	−2.33			−2.99
TRINITY_DN21137_c0_g1	GID1C	Gibberellin receptor GID1C					2.77	7.5
TRINITY_DN37680_c0_g1	JMJ14	Probable lysine-specific demethylase JMJ14						11.2
TRINITY_DN7266_c0_g2	LD	Homeobox protein LUMINIDEPENDENS	2.16		2.68		3.09	7.25
TRINITY_DN6935_c0_g1	MSI4	WD-40 repeat-containing protein MSI4						10.21
TRINITY_DN34495_c0_g1	NFYB2	Nuclear transcription factor Y subunit B-2			2.4	2.58	2.59	
TRINITY_DN18038_c0_g1	NFYB3	Nuclear transcription factor Y subunit B-3					2.17	8.27
TRINITY_DN35701_c0_g2	NFYC1	Nuclear transcription factor Y subunit C-1						2.59
TRINITY_DN1267_c0_g1	PEX4	Pollen-specific leucine-rich repeat extensin-like protein 4	−8.5	−5.05	−5.26	−8.04	−4.31	−3.62
TRINITY_DN6353_c0_g1	PHYA	Phytochrome A			2.15	2.39		
TRINITY_DN21387_c0_g1	PHYB	Phytochrome B	−2.28					
TRINITY_DN7954_c0_g1	PI	Floral homeotic protein PISTILLATA	−8.44	−6.51	−7.06	−8.3	−3.54	−3.36
TRINITY_DN12744_c0_g2	SEP1	Developmental protein SEPALLATA 1	−7.94	−7.09	−7.56	−8.08	−2.8	
TRINITY_DN31040_c0_g1	SEP3	Developmental protein SEPALLATA 3					−2.37	
TRINITY_DN2251_c0_g1	SOC1	MADS-box protein SOC1	4.05	2.9	3.46	3.1	2.6	12.47
TRINITY_DN6192_c0_g1	SPL15	Squamosa promoter-binding-like protein 15						10.17
TRINITY_DN6705_c0_g1	SPL3	Squamosa promoter-binding-like protein 3	−3.84		−3.38	−4.54		−2.82
TRINITY_DN14821_c0_g1	SPL4	Squamosa promoter-binding-like protein 4		−3.38	−2.18			
TRINITY_DN57302_c0_g1	SRF6	Protein STRUBBELIG-RECEPTOR FAMILY 6	−4.07	−3.28	−4.01	−3.91		
TRINITY_DN46547_c0_g1	SRF8	Protein STRUBBELIG-RECEPTOR FAMILY 8						7.42
TRINITY_DN2130_c0_g1	SRR1	Protein SENSITIVITY TO RED LIGHT REDUCED 1						12.09
TRINITY_DN29363_c0_g1	SVP	MADS-box protein SVP						−3.8
TRINITY_DN5406_c1_g1	UBC1	Ubiquitin-conjugating enzyme E2 1						7.86

Table 4. *Cont.*

Gene ID	Gene Name	Protein Name	Log2FC					
			M1a1	**M1a2**	**M1o1**	**M1o2**	**M2a4**	**M2o4**
TRINITY_DN16649_c0_g1	*ULT1*	Protein ULTRAPETALA 1					−2.18	
TRINITY_DN13113_c0_g1	*VRN1*	B3 domain-containing transcription factor VRN1	−3.2	−2.14	−2.41	−2.73		
TRINITY_DN8011_c0_g1	*WNK1*	Serine/threonine-protein kinase WNK1						8.81

In all comparisons, TFs potentially related to male sterility were mostly associated with down-regulated DEGs (Figure 3). These TFs were classified into 10 major families, namely *AP2/ERF*, *bHLH*, *bZIP*, *C2C2*, *C2H2*, *HB*, *MADS*, *MYB*, *NAC*, and *WRKY*, from which the most representative families in all comparisons were *WRKY* and *MYB*. These TFs were particularly abundant in DEGs in M2o4 and particularly low in M2d4. Furthermore, TFs from apomictic DEGs showed an enrichment of metabolic pathways in the KEGG database. "Plant hormone signal transduction" (KEGG:04075) was up-regulated in M1o1 and M2o4, showing both up- and down-regulation in M1o2 and in M2a4, involving two *AHK*, *ARF1*, two *ARR*, *BZR2*, *DPBF3*, *EIN4*, *ERF2*, *ETR1*, *GBF4*, four *IAA*, *MYC2*, *NPR5* and three *TGA*. Up-regulation of "Lysine degradation" (KEGG:00310) and "MAPK signaling pathway—plant" (KEGG:04016) were only enriched in M2o4. The first was associated with *ASHR1*, two *ATXR*, *EZA1*, two *SUVH* and *SUVR3*, while the second involved *EIN4*, *ETR1*, *MYC2* and two *WRKY*. Moreover, WikiPathways "flower development" (WP:WP618) and "flower development (initiation)" (WP:WP2108) were enriched among up-DEGs across comparisons, being related to AG, three *AP*, *PI*, *RAP2-7*, two *SEP*, *SOC1*, and *SVP* (Supplementary Table S10).
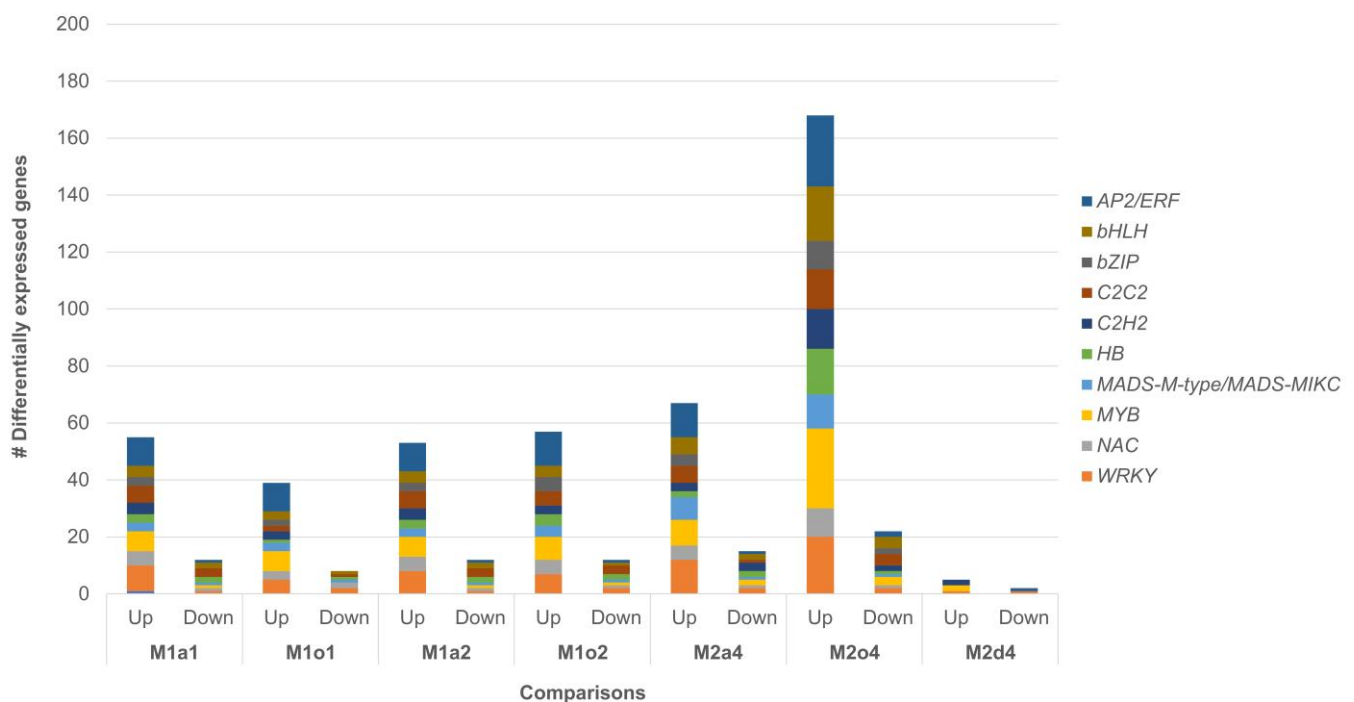
Figure 3. Distribution of differentially expressed transcription factors potentially related to male sterility is classified into the 10 families with the highest number of differentially expressed genes (DEGs) in ovules: Apomictic *L. multiflorum* (M), sexual *L. auriculifolium* (a) and *L. ovalifolium* (o), and facultative apomictic *L. dodartii*: *AP2/ERF*, *bHLH*, *bZIP*, *C2C2*, *C2H2*, *HB*, *MADS*, *MYB*, *NAC*, and *WRKY*.

Additionally, four DEGs were found to be associated with tryptophan metabolism, namely *TAA1*, *TSB2*, and AT3G04600, which were up-regulated in M2o4 and TAR2, which

was down-regulated in most comparisons (Table 5). Moreover, 29 DEGs were found to be related to ethylene, namely *AIL5*, *ANT*, *CRF2*, *EIN2*, 14 *ERF*, *ERS1*, five *RAP2*, *RTE1*, *SHN3*, *TINY*, *WR11*, and AT4G13040, the majority of which were up-regulated in apomictic plants, especially in M2o4. Furthermore, 12 DEGs were found to be related to aminoacyl-tRNA, namely *AO*, *EDD1*, *GDH2*, two *GLDP*, *GRDP2*, *PSS1*, three *RBG*, *RZ1A*, and *UGLYAH*, which showed a similar regulation. Furthermore, 29 DEGs were found to be related to lysine, namely *AATL1*, *ASHR1*, three *ATX*, four *ATXR*, *ELF6*, *EMB3003*, *EZA1*, three *JMJ*, two *LHT*, *LTA2*, *OVA5*, two *SUVH*, three *SUVR*, AT1G25530, AT4G26910, AT5G55070, AT4G35180, and AT3G11710, presenting mostly up-regulation in apomictic plants (Table 5).

Table 5. List of differentially expressed genes (DEGs) in ovules of *Limonium* plants, namely apomictic *L. multiflorum* (M) relative to sexual *L. auriculifolium* (a) and *L. ovalifolium* (o), in different stages, which are involved in tryptophan, ethylene, aminoacyl-tRNA, or lysine metabolism. DEGs were filtered by |log2 fold-change (log2FC)| > 2. DEGs were mapped to their respective *A. thaliana* homolog (gene name) and annotated according to its reference genome (red: up-regulated DEGs; blue: down-regulated DEGs).

Gene ID	Gene Name	Protein Name	Log2FC						
			M1a1	M1a2	M1o1	M1o2	M2a4	M2o4	M2d4
		Aminoacyl-tRNA							
TRINITY_DN2761_c0_g1	*AO*	L-aspartate oxidase, chloroplastic	2.11		2.61				
TRINITY_DN4987_c0_g1	*EDD1*	Glycine–tRNA ligase, chloroplastic/mitochondrial 2						12.19	
TRINITY_DN157005_c0_g1	*GDH2*	Glycine cleavage system H protein 2, mitochondrial	−3.49	−2.94	−2.46	−2.49	−2.5		
TRINITY_DN2155_c4_g1	*GLDP1*	Glycine dehydrogenase (decarboxylating) 1, mitochondrial						2.29	
TRINITY_DN10603_c0_g1	*GLDP2*	Glycine dehydrogenase (decarboxylating) 2, mitochondrial		4.14				7.09	
TRINITY_DN2985_c0_g1	*GRDP2*	Glycine-rich domain-containing protein 2							−2.18
TRINITY_DN6537_c0_g1	*PSS1*	CDP-diacylglycerol–serine O-phosphatidyltransferase 1					9.39		
TRINITY_DN20064_c0_g1	*RBG3*	Glycine-rich RNA-binding protein 3, mitochondrial							−2.44
TRINITY_DN8570_c0_g1	*RBG4*	Glycine-rich RNA-binding protein 4, mitochondrial					3.75	8.48	
TRINITY_DN8373_c0_g1	*RBG5*	Glycine-rich RNA-binding protein 5, mitochondrial						9.41	
TRINITY_DN27069_c0_g1	*RZ1A*	Glycine-rich RNA-binding protein RZ1A						2.24	
TRINITY_DN14144_c0_g1	*UGLYAH*	(S)-ureidoglycine aminohydrolase	2.79			2.01	3.21	7.94	
		Ethylene							
TRINITY_DN15258_c0_g1	*AIL5*	AP2-like ethylene-responsive transcription factor AIL5	−2.78	−3.27	−3.23	−2.23		8.8	
TRINITY_DN51613_c0_g1	*ANT*	AP2-like ethylene-responsive transcription factor ANT						6.87	
TRINITY_DN13736_c0_g1	*CRF2*	Ethylene-responsive transcription factor CRF2					−3.02	−2.65	
TRINITY_DN68_c0_g2	*EIN2*	Ethylene-insensitive protein 2		2.15	2.3			11.11	
TRINITY_DN2468_c0_g1	*ERF010*	Ethylene-responsive transcription factor ERF010						3.25	
TRINITY_DN9993_c0_g1	*ERF014*	Ethylene-responsive transcription factor ERF014						−2.01	
TRINITY_DN1685_c1_g1	*ERF018*	Ethylene-responsive transcription factor ERF018		2.98	3.3	3.09		2.52	
TRINITY_DN18951_c0_g1	*ERF034*	Ethylene-responsive transcription factor ERF034						−3.47	
TRINITY_DN7978_c0_g2	*ERF054*	Ethylene-responsive transcription factor ERF054	3.29		3.21	4.29	3.91	10.81	
TRINITY_DN455_c0_g2	*ERF061*	Ethylene-responsive transcription factor ERF061		2.36				10.86	
TRINITY_DN74944_c0_g3	*ERF071*	Ethylene-responsive transcription factor ERF071						−2.59	

Table 5. *Cont.*

Gene ID	Gene Name	Protein Name	Log2FC						
			M1a1	M1a2	M1o1	M1o2	M2a4	M2o4	M2d4
TRINITY_DN2504_c1_g1	*ERF109*	Ethylene-responsive transcription factor ERF109	2.63			3.22	4.14	10.25	
TRINITY_DN12655_c0_g1	*ERF114*	Ethylene-responsive transcription factor ERF114						9.96	
TRINITY_DN40207_c0_g1	*ERF118*	Ethylene-responsive transcription factor ERF118					−2.01		
TRINITY_DN15135_c0_g1	*ERF1A*	Ethylene-responsive transcription factor 1A						11.43	
TRINITY_DN5700_c2_g1	*ERF2*	Ethylene-responsive transcription factor 2					2.19	10.77	
TRINITY_DN10435_c0_g1	*ERF5*	Ethylene-responsive transcription factor 5		7.93	7.95			7.89	
TRINITY_DN4039_c0_g2	*ERF9*	Ethylene-responsive transcription factor 9						2.46	
TRINITY_DN9095_c0_g1	*ERS1*	Ethylene response sensor 1						9.71	
TRINITY_DN2665_c0_g1	*RAP2-13*	Ethylene-responsive transcription factor RAP2-13						10.11	
TRINITY_DN40774_c0_g3	*RAP2-3*	Ethylene-responsive transcription factor RAP2-3	−5.92	−4.04	−5.69	−5.82		−2.5	
TRINITY_DN1497_c0_g1	*RAP2-4*	Ethylene-responsive transcription factor RAP2-4						4.08	
TRINITY_DN2_c1_g1	*RAP2-6*	Ethylene-responsive transcription factor RAP2-6			2.25	2.3	2.41	11.76	
TRINITY_DN12350_c0_g1	*RAP2-7*	Ethylene-responsive transcription factor RAP2-7	6.43	4.91	6.54	4.61	4.12	9.24	
TRINITY_DN5947_c0_g1	*RTE1*	Protein REVERSION-TO-ETHYLENE SENSITIVITY1						10.91	
TRINITY_DN29694_c0_g1	*SHN3*	Ethylene-responsive transcription factor SHINE 3					−3.72	−3.93	
TRINITY_DN4330_c3_g1	*TINY*	Ethylene-responsive transcription factor TINY						9.64	
TRINITY_DN148_c3_g1	*WRI1*	Ethylene-responsive transcription factor WRI1	−2.13			−2.63			
TRINITY_DN5382_c0_g1	*AT4G13040*	Ethylene-responsive transcription factor-like protein At4g13040						9.5	
		Lysine							
TRINITY_DN6270_c0_g1	*AATL1*	Lysine histidine transporter-like 8						2.04	
TRINITY_DN8133_c0_g1	*ASHR1*	Histone-lysine N-methyltransferase ASHR1						10.07	
TRINITY_DN4218_c0_g3	*ATX2*	Histone-lysine N-methyltransferase ATX2						7.65	−3.53
TRINITY_DN3010_c0_g1	*ATX4*	Histone-lysine N-methyltransferase ATX4						11.71	
TRINITY_DN209_c0_g2	*ATX5*	Histone-lysine N-methyltransferase ATX5					7.64	7.46	
TRINITY_DN1076_c0_g1	*ATXR2*	Histone-lysine N-methyltransferase ATXR2						10.78	
TRINITY_DN1656_c0_g1	*ATXR3*	Histone-lysine N-methyltransferase ATXR3						2.13	
TRINITY_DN11945_c0_g1	*ATXR4*	Histone-lysine N-methyltransferase ATXR4						9.06	
TRINITY_DN15991_c0_g1	*ATXR5*	Histone-lysine N-methyltransferase ATXR5					−3.1	6.81	
TRINITY_DN22923_c0_g1	*ELF6*	Probable lysine-specific demethylase ELF6						5.1	
TRINITY_DN6877_c1_g1	*EMB3003*	Dihydrolipoyllysine-residue acetyltransferase component 5 of pyruvate dehydrogenase complex. chloroplastic						−2.46	
TRINITY_DN14929_c0_g1	*EZA1*	Histone-lysine N-methyltransferase EZA1						2.92	
TRINITY_DN37680_c0_g1	*JMJ14*	Probable lysine-specific demethylase JMJ14						11.2	
TRINITY_DN3464_c0_g3	*JMJ25*	Lysine-specific demethylase JMJ25						8.39	
TRINITY_DN3267_c0_g1	*JMJ30*	Lysine-specific demethylase JMJ30			−2.4	−2.16		9.65	
TRINITY_DN1796_c2_g1	*LHT1*	Lysine histidine transporter 1	4.61	3.22	2.51	3.81	4.38	10.07	
TRINITY_DN1796_c0_g3	*LHT2*	Lysine histidine transporter 2						9.7	
TRINITY_DN6877_c1_g2	*LTA2*	Dihydrolipoyllysine-residue acetyltransferase component 4 of pyruvate dehydrogenase complex. chloroplastic	−2.23						
TRINITY_DN92_c0_g1	*OVA5*	Lysine–tRNA ligase. chloroplastic/mitochondrial						2.08	
TRINITY_DN22984_c0_g1	*SUVH6*	Histone-lysine N-methyltransferase. H3 lysine-9 specific SUVH6					−2.35	7.17	
TRINITY_DN393_c0_g2	*SUVH9*	Histone-lysine N-methyltransferase family member SUVH9						10.36	
TRINITY_DN18492_c0_g1	*SUVR1*	Probable inactive histone-lysine N-methyltransferase SUVR1						10.33	
TRINITY_DN10785_c0_g1	*SUVR3*	Histone-lysine N-methyltransferase SUVR3						7.14	
TRINITY_DN27123_c0_g1	*SUVR4*	Histone-lysine N-methyltransferase SUVR4						9.46	
TRINITY_DN22651_c0_g1	*AT1G25530*	Lysine histidine transporter-like 6						10.9	2.27

Table 5. *Cont.*

Gene ID	Gene Name	Protein Name	Log2FC						
			M1a1	M1a2	M1o1	M1o2	M2a4	M2o4	M2d4
TRINITY_DN21036_c0_g1	*AT4G26910*	Dihydrolipoyllysine-residue succinyltransferase component of 2-oxoglutarate dehydrogenase complex 2. mitochondrial						9.63	
TRINITY_DN1947_c0_g1	*AT5G55070*	Dihydrolipoyllysine-residue succinyltransferase component of 2-oxoglutarate dehydrogenase complex 1. mitochondrial						9.52	
TRINITY_DN971_c1_g3	*AT4G35180*	Lysine histidine transporter-like 7						8.3	
TRINITY_DN40168_c0_g1	*AT3G11710*	Lysine–tRNA ligase. cytoplasmic						7.18	
		Tryptophan							
TRINITY_DN10705_c0_g1	*TAA1*	L-tryptophan–pyruvate aminotransferase 1						7.41	
TRINITY_DN6324_c0_g2	*TAR2*	Tryptophan aminotransferase-related protein 2	−4.07	−2.65	−3.72	−4.13	−3.64		
TRINITY_DN18489_c0_g3	*TSB2*	Tryptophan synthase β chain 2. chloroplastic					2.13	7.83	
TRINITY_DN257_c0_g2	*AT3G04600*	Tryptophan–tRNA ligase. cytoplasmic						10.25	

3.5. General GO Enrichment

DEGs between apomictic and sexual ovules in early stages were found to be enriched in seven main ancestor terms (Figure 4A). Most biological regulation terms (GO:0032501, GO:0048580, GO:2000241) were mainly enriched in up-DEGs in M1o2, although "regulation of flower development" (GO:0009909) was enriched in down-DEGs (Figure 4A). Cellular processes (GO:0007015, GO:0030029) were enriched among down-DEGs of M1o1 and M1o2. Although some developmental processes (GO:0009653, GO:0010623) were enriched among down-DEGs, "flower development" (GO:0009908) was enriched among up-DEGs. Localization terms related to biomolecules (GO:0015800, GO:0008643) were down-regulated, while transmembrane transports (GO:1903959, GO:0055085) were up-regulated in M1a1 and M1a2, but mainly down-regulated in M1o1 and M1o2. Although several metabolic processes (GO:0006631, GO:0045490, GO:0009699, GO:0000272, GO:0006468) were down-regulated, photosynthesis-related processes (GO:0005996, GO:0015979, GO:0019684) were up-regulated. Most responses to stimuli (GO:0009416, GO:0014070, GO:0006979) were enriched in up-DEGs. Finally, signaling terms (GO:0023052, GO:0007166) were mainly up-regulated (Figure 4A).

DEGs from M2a4 and M2o4 showed many enriched terms, especially in the up-DEGs of the latter. DEGs from M2d4 presented only six enriched metabolic process terms associated with down-regulated DEGs (Figure 4B). Most biological regulation terms (GO:0010629, GO:0048522, GO:0010646, GO:0009966, GO:0023051, GO:0010119) were enriched among up-regulated DEGs from M2o4, while "regulation of pollen tube growth" (GO:0080092) was down-regulated in M2a4. Although most cellular process terms were up-regulated in M2o4 (GO:0007049, GO:0051301, GO:0071840, GO:0007059, GO:0051321, GO:0090332, GO:0010118), they were down-regulated in M2a4 (GO:0071840, GO:0032501, GO:0009826). "Callose localization" (GO:0052545) was only enriched for down-DEGs in M2o4. Reproductive processes presented both types of regulation, where "pollination" (GO:0009856) and "pollen tube development" (GO:0080092) were down-regulated in M2o4 and M2a4, respectively, but "reproductive structure development" (GO:0048868) was enriched among up-DEGs in M2a4. Metabolic process and response to stimulus terms were mainly enriched in up-DEGs from apomictic ovules relative to both sexual species (Figure 4B).
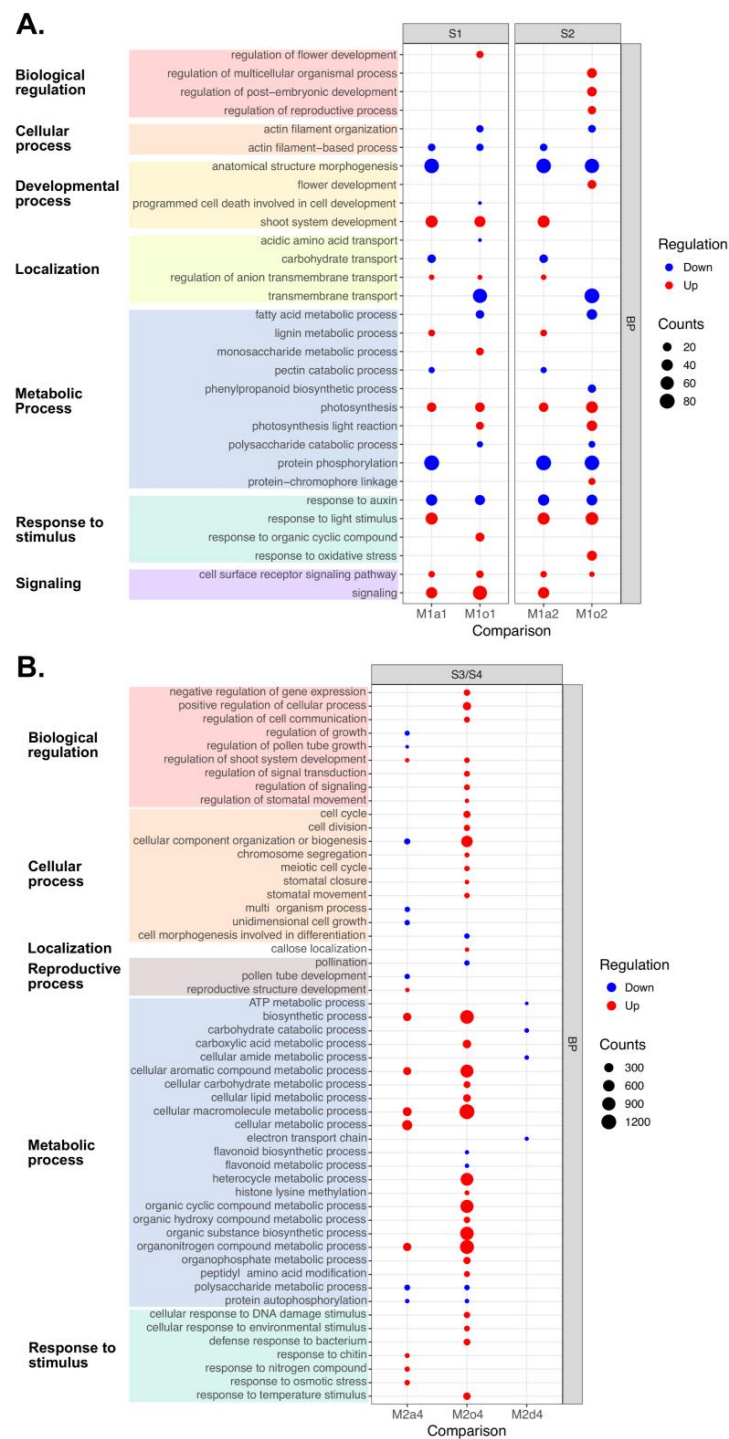
Figure 4. Over-representation analysis (ORA) performed by gProfiler of differentially expressed genes (DEGs) in ovules from apomictic *L. multiflorum* (M), sexual *L. auriculifolium* (a) and *L. ovalifolium* (o), and facultative apomictic *L. dodartii*. DEGs were filtered by |log2 fold-change (log2FC)| >2. *A.s thaliana*, the most similar homolog of each differentially expressed gene (DEG) was mapped to the respective functional annotation, and enriched terms were summarized using REVIGO. Significantly (FDR < 0.01), gene ontology (GO) and biological processes (BP) terms are among DEGs from (**A**) apomictic in S1 relative to sexual ovules in S1 (M1a1 and M1o1) or S2 (M1a2 and M1o2), and from (**B**) apomictic in S2 relative to sexual ovules in S3/S4 (M2a4 and M2o4), and facultative apomictic in S4 (M2d4). The dot's size indicates the number of DEGs annotated with each term (counts), and the color shows the differential expression (red: up-regulated; blue: down-regulated). Enriched terms are grouped by their respective ancestors (ontology level 2).

3.6. GO Enrichment in Floral and Pollen-Related DEGs

Among all DEGs, 49 were found to be floral-related, which were mainly up-regulated for flowering and gibberellin-related terms (GO:0009908, GO:0010228, GO:0009685, GO:0010077, GO:0009739, GO:0048573, GO:0048437; Figure 5). Conversely, there was a predominance of down-regulation in DEGs related to brassinosteroid, ovule and inflorescence development, and floral organ identity (GO:0010268, GO:0009741, GO:0048481, GO:0010229, GO:0010093).
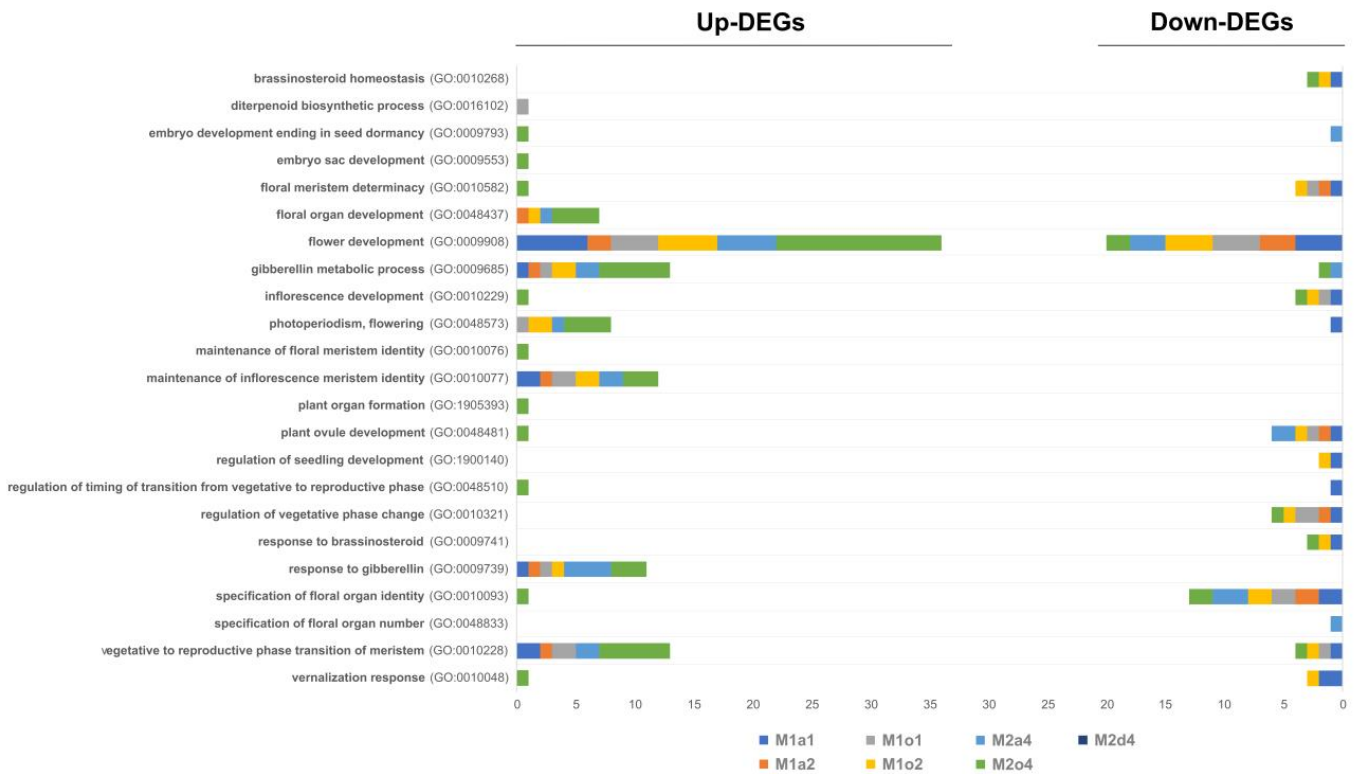
Figure 5. Regulation of up- and down-regulated differentially expressed genes (DEGs) in ovules in stages S1 (1), S2 (2), and S3/S4 (4) from apomictic *L. multiflorum* (M), sexual *L auriculifolium* (a) and *L. ovalifolium* (o), and facultative apomictic *L. dodartii* (d), annotated with female-related Gene Ontology (GO) terms. DEGs represent the number of significant genes found to be differently expressed in each comparison.

Overall, among DEGs annotated with pollen-related GO terms, the majority were downregulated in all comparisons (Figure 6; Table 6). However, "pollen development" (GO:0009555), "pollen maturation" (GO:0010152), "pollen tube" (GO:0090406), "pollen tube growth" (GO:0009860) and "pollen tube guidance" (GO:0010183) were up-regulated in M2o4. Globally, both up- and down-regulated DEGs were especially related to pollen development. Noticeably, down-regulated DEGs were also related to pollen wall assembly and pollen tube development and growth. Specifically, the *EX5* gene was found to be down-regulated in M1a1 and M1o2.
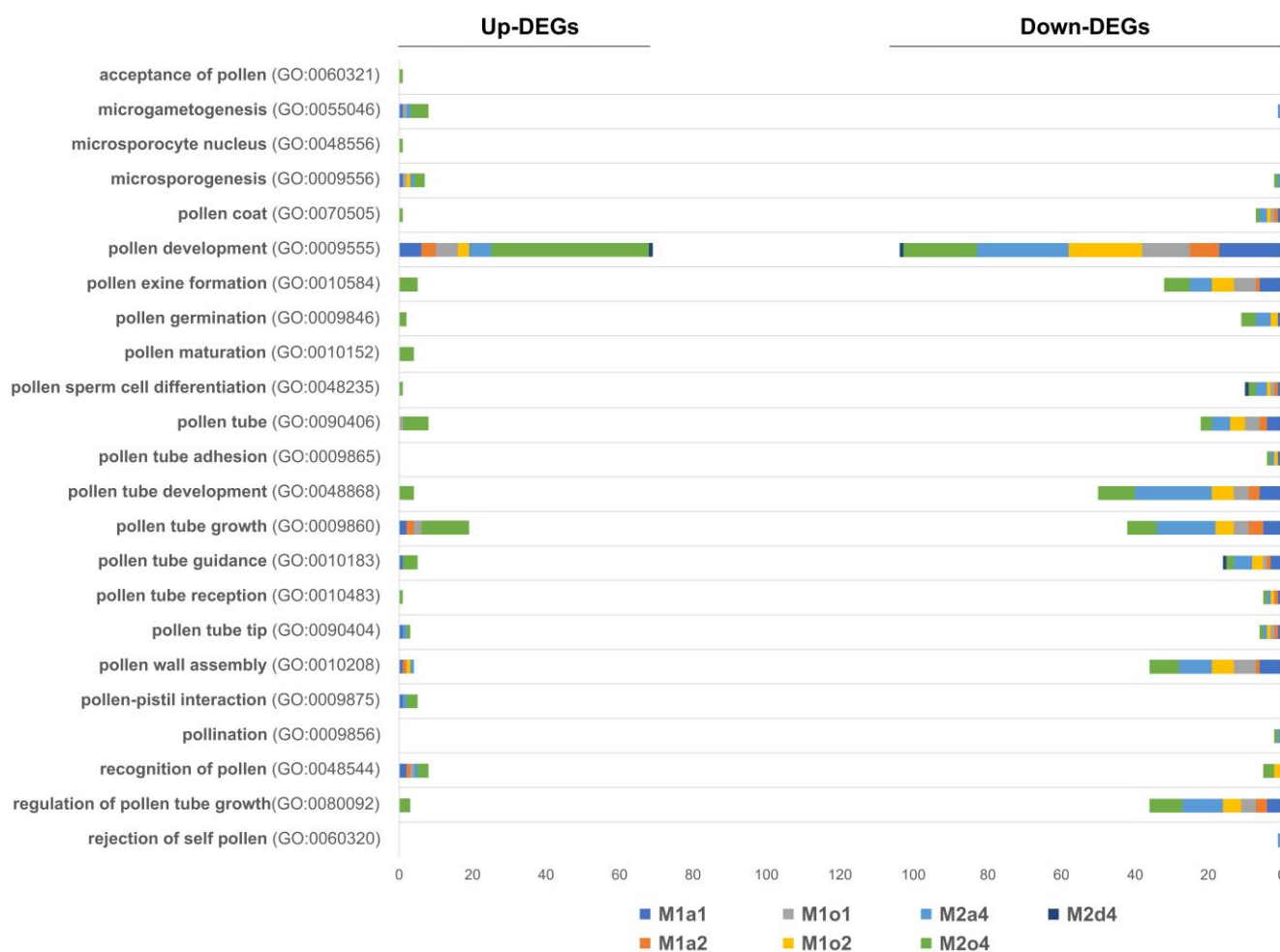
Figure 6. Regulation of up- and down-regulated differentially expressed genes (DEGs) in ovules in stages S1 (1), S2 (2), and S3/S4 (4) from apomictic *L. multiflorum* (M), sexual *L auriculifolium* (a) and *L. ovalifolium* (o), and facultative apomictic *L. dodartii* (d), annotated with Gene Ontology (GO) terms related to pollen. DEGs represent the number of significant genes found to be differently expressed in each comparison.

Table 6. Changes in expression of uniquely annotated differentially expressed genes (DEGs) related to pollen from ovules of apomictic *L. multiflorum* (M) in S1 (1) relative to sexual *L. auriculifolium* (a) and *L. ovalifolium* (o) in either S1 (1) or S2 (2), and *L. multiflorum* (M) in S2 (2) relative to *L. auriculifolium* (a), *L. ovalifolium* (o), and facultative apomictic *L. dodartii* (d) in S3/S4 (4). Annotated DEGs according to *A. thaliana* homologs (gene names) were searched in biological process (BP), molecular function (MF), and cellular component (CC) Gene Ontology (GO) terms related to pollen (red: up-regulated DEGs; blue: down-regulated DEGs).

Gene ID	Gene Name	Protein Name	M1a1	M1a2	M1o1	M1o2	M2a4	M2o4	M2d4
		pollen development (GO:0009555)							
TRINITY_DN5448_c0_g1	*NAS3*	Nicotianamine synthase 3	−3.49	−4.95	−3.84	−3.52			
TRINITY_DN95402_c0_g1	*PS1*	FHA domain-containing protein PS1	−2.61			−2.08	−2.42	8.49	
TRINITY_DN38119_c0_g1	*KDSB*	3-deoxy-manno-octulosonate cytidylyltransferase, mitochondrial	2.07						
TRINITY_DN10816_c0_g1	*TMK3*	Receptor-like kinase TMK3	−3.51			−2.75	−2.57	−3.57	
TRINITY_DN923_c0_g1	*CALS5*	Callose synthase 5	−2.91		−2.05	−3.3	−3.49		
TRINITY_DN111580_c0_g2	*CYP73A5*	Trans-cinnamate 4-monooxygenase	2.6	2.57	3.63	2.01			
TRINITY_DN41226_c0_g1	*PAL1*	Phenylalanine ammonia-lyase 1	−2.27			−2.65		−3.8	
TRINITY_DN2633_c0_g1	*CALS9*	Callose synthase 9	2.08				2.07	9.17	
TRINITY_DN1417_c2_g1	*FAB1B*	1-phosphatidylinositol-3-phosphate 5-kinase FAB1B	2.35		2.38	2.68		3.2	

Table 6. *Cont.*

Gene ID	Gene Name	Protein Name	M1a1	M1a2	M1o1	M1o2	M2a4	M2o4	M2d4
TRINITY_DN1233_c4_g1	AT4G39110	Probable receptor-like protein kinase At4g39110	−8.01	−4.86	−4.65	−7.56	−4.44	−3.74	
TRINITY_DN3115_c1_g1	ATL73	RING-H2 finger protein ATL73	−2.87	−2.93	−2.79	−2.45		8.09	
TRINITY_DN6027_c0_g1	LRP1	Protein LATERAL ROOT PRIMORDIUM 1	−2.64	−2.92	−2.65	−2.47			
TRINITY_DN5863_c0_g1	LCB2A	Long chain base biosynthesis protein 2a	2.81						
TRINITY_DN7884_c0_g1	XRI1	Protein XRI1	−4.22				−3.9	−2.9	
TRINITY_DN4445_c0_g1	CEP1	KDEL-tailed cysteine endopeptidase CEP1	−6.27	−7.42	−6.31	−5.23			
TRINITY_DN8949_c0_g1	SWEET13	Bidirectional sugar transporter SWEET13	−2.61	−2.07		−2.58			
TRINITY_DN10107_c0_g1	ABCB25	ABC transporter B family member 25, mitochondrial	2.48		2.73			2.35	8.62
TRINITY_DN27954_c0_g3	LECRK42	L-type lectin-domain containing receptor kinase IV.2		3.43				−2.54	−3.02
TRINITY_DN8056_c1_g1	CALS11	Callose synthase 11		3.3	3.44		3.29	8.01	
TRINITY_DN4094_c0_g1	NMT1	Phosphoethanolamine N-methyltransferase 1		2.15	2.43				
TRINITY_DN17932_c0_g1	WRKY2	Probable WRKY transcription factor 2			−2.02	−2.22	−2.23	7.15	
TRINITY_DN12987_c0_g1	PIN5	Auxin efflux carrier component 5		2.41				10	3.48
TRINITY_DN4445_c0_g1	CEP1	KDEL-tailed cysteine endopeptidase CEP1							
TRINITY_DN5448_c0_g1	NAS3	Nicotianamine synthase 3							
TRINITY_DN3873_c0_g1	AGL65	Agamous-like MADS-box protein AGL65				−2.29	−2.62	−3.28	
TRINITY_DN47156_c0_g1	IPK2B	Inositol polyphosphate multikinase β					3.28	7.44	
TRINITY_DN2407_c1_g1	BZIP34	Basic leucine zipper 34					−5.18	−2.68	
TRINITY_DN12180_c0_g1	AGL66	Agamous-like MADS-box protein AGL66					−4.72	−3.81	
TRINITY_DN15991_c0_g1	ATXR5	Histone-lysine N-methyltransferase ATXR5					−3.1	6.81	
TRINITY_DN9971_c0_g1	MYB80	Transcription factor MYB80					4.46	8.63	
TRINITY_DN10584_c0_g1	MCM7	DNA replication licensing factor MCM7					−2.04		
TRINITY_DN5641_c0_g1	LOX3	Lipoxygenase 3, chloroplastic					2.93	2.75	
TRINITY_DN23341_c0_g1	D6PKL3	Serine/threonine-protein kinase D6PKL3					2.16	8.44	
TRINITY_DN11273_c0_g1	MCM4	DNA replication licensing factor MCM4						−4.4	
TRINITY_DN440_c0_g1	MCM8	Probable DNA helicase MCM8						12.61	
TRINITY_DN3132_c0_g1	PGDH1	D-3-phosphoglycerate dehydrogenase 1, chloroplastic						11.73	
TRINITY_DN12133_c0_g1	MRS2-2	Magnesium transporter MRS2-2						11.26	
TRINITY_DN7153_c0_g1	APD2	E3 ubiquitin-protein ligase APD2						11.16	
TRINITY_DN4731_c0_g3	MYB101	Transcription factor MYB101						11.05	
TRINITY_DN1371_c0_g1	RGTB1	Geranylgeranyl transferase type-2 subunit β 1						11.03	
TRINITY_DN2976_c0_g1	AT2G21870	Probable ATP synthase 24 kDa subunit. mitochondrial						9.59	
TRINITY_DN11362_c1_g1	WRKY35	Probable WRKY transcription factor 35						9.53	
TRINITY_DN166676_c0_g1	CER26L	Protein ECERIFERUM 26-like						9.43	
TRINITY_DN9251_c0_g1	FAS1	Chromatin assembly factor 1 subunit FAS1						9.15	
TRINITY_DN17928_c0_g2	CYP94B3	Cytochrome P450 94B3						−2.3	
TRINITY_DN1593_c0_g1	DSE1	Protein DECREASED SIZE EXCLUSION LIMIT 1						3.87	
TRINITY_DN41732_c1_g1	GAPCP1	Glyceraldehyde-3-phosphate dehydrogenase GAPCP1, chloroplastic						−2.38	
TRINITY_DN968_c1_g1	CDKA-1	Cyclin-dependent kinase A-1						8.61	
TRINITY_DN114534_c0_g1	LCB2B	Long chain base biosynthesis protein 2b						8.44	
TRINITY_DN39521_c0_g1	RUK	Serine/threonine-protein kinase RUNKEL						8.41	
TRINITY_DN30938_c0_g1	XPO1	Protein EXPORTIN 1A						2.82	
TRINITY_DN54834_c0_g2	KIN7A	Kinesin-like protein KIN-7A						7.81	
TRINITY_DN29594_c0_g1	PTD	Protein PARTING DANCERS						7.27	
TRINITY_DN3033_c0_g4	P5CSA	Delta-1-pyrroline-5-carboxylate synthase A						2.7	
TRINITY_DN31412_c0_g1	RGP1	UDP-arabinopyranose mutase 1						7.16	
TRINITY_DN14808_c0_g1	RTEL1	Regulator of telomere elongation helicase 1 homolog						6.99	
TRINITY_DN49207_c0_g1	SRS1	Protein SHI RELATED SEQUENCE 1						6.96	
TRINITY_DN29704_c0_g5	SRS5	Protein SHI RELATED SEQUENCE 5						6.81	
TRINITY_DN9646_c0_g1	ATRX	Protein CHROMATIN REMODELING 20						2.32	
TRINITY_DN21539_c0_g1	BHLH91	Transcription factor bHLH91						6.74	

Table 6. *Cont.*

Gene ID	Gene Name	Protein Name	M1a1	M1a2	M1o1	M1o2	M2a4	M2o4	M2d4
TRINITY_DN826_c0_g2	TULP7	Tubby-like F-box protein 7						2.15	
TRINITY_DN4508_c0_g1	MPK4	Mitogen-activated protein kinase 4						2.09	
TRINITY_DN161_c0_g2	NEDD1	Protein NEDD1						2.22	
TRINITY_DN6156_c0_g1	PKSA	Type III polyketide synthase A	−3.61		−6.78	−6.63	−3.39	−2.98	
TRINITY_DN31801_c4_g1	GPAT1	Glycerol-3-phosphate acyltransferase 1					−4.13	−4.38	
TRINITY_DN17166_c0_g1	4CL3	4-coumarate–CoA ligase 3	−4.44		−2.69	−4.06	−3.78	−2.43	
TRINITY_DN16998_c0_g1	ZAT2	Zinc finger protein ZAT2					−4.9	−4.15	
TRINITY_DN15578_c0_g1	LRL1	Transcription factor LRL1					−3.39	6.94	
TRINITY_DN4588_c0_g2	ABCG31	ABC transporter G family member 31	−2.72	−3.81	−2.13	−2.53	−2.22	10.04	
TRINITY_DN45712_c0_g1	FAR2	Fatty acyl-CoA reductase 2, chloroplastic	−3.28		−6.24	−6.93	−4.07	−2.8	
TRINITY_DN9952_c0_g1	ABCG26	ABC transporter G family member 26					−3.28		
TRINITY_DN15838_c0_g1	TIP5-1	Probable aquaporin TIP5-1				−2.48	−2.82	8.26	
TRINITY_DN6869_c0_g1	A6	Probable glucan endo-1,3-β-glucosidase A6	−2.6		−7.57	−7.88	−2.61	−2.95	
TRINITY_DN156774_c0_g1	ABCG9	ABC transporter G family member 9					−2.19	−3.86	
TRINITY_DN31379_c0_g1	TKPR1	Tetraketide α-pyrone reductase 1					−4.21	−4.43	
TRINITY_DN3196_c3_g1	EMS1	Leucine-rich repeat receptor protein kinase EMS1					−2.05	−2.34	
TRINITY_DN176325_c0_g1	COPT1	Copper transporter 1	−3.79	−3.86	−3.99	−3.76	−2.12		
TRINITY_DN4485_c0_g1	CYP704B1	Cytochrome P450 704B1						−2.52	
		microsporogenesis (GO:0009556)							
TRINITY_DN5204_c0_g1	PLC2	Phosphoinositide phospholipase C 2	3.07		2.44	3.37	2.07	3.53	
TRINITY_DN3196_c3_g1	EMS1	Leucine-rich repeat receptor protein kinase EMS1					−2.05	−2.34	
TRINITY_DN6537_c0_g1	PSS1	CDP-diacylglycerol–serine O-phosphatidyltransferase 1						9.39	
TRINITY_DN2003_c0_g1	FH14	Formin-like protein 14						2.33	
		pollen germination (GO:0009846)							
TRINITY_DN373_c0_g1	CSLD1	Cellulose synthase-like protein D1	−3.31			−4.72	−3.45	−2.22	
TRINITY_DN19056_c0_g1	IP5P13	Type I inositol polyphosphate 5-phosphatase 13				−2.38	−3.35	−2.36	
TRINITY_DN4602_c0_g1	JGB	Protein JINGUBANG					−4	−4.06	
TRINITY_DN8465_c0_g1	CSLD4	Cellulose synthase-like protein D4					−3.89	−3.71	
TRINITY_DN46361_c0_g1	PTF2	Plant-specific TFIIB-related protein PTF2						9.36	
TRINITY_DN19056_c0_g3	IP5P12	Type I inositol polyphosphate 5-phosphatase 12						6.94	
		pollination (GO:0009856)							
TRINITY_DN6022_c0_g1	ARPN	Basic blue protein					−5.23	−3.65	
		pollen tube growth (GO:0009860)							
TRINITY_DN8457_c0_g3	AT1G03010	BTB/POZ domain-containing protein At1g03010	−4.41	−4.84	−4.35	−3.42		2.01	
TRINITY_DN5849_c0_g1	XI-E	Myosin-11	2.14	4.3	3.52			7.48	
TRINITY_DN691_c0_g2	ARAC5	Rac-like GTP-binding protein ARAC5	−3.62	−2.02	−2.9	−3.64	−2.65		
TRINITY_DN11455_c0_g1	CBL1	Calcineurin B-like protein 1	2.24					4.42	
TRINITY_DN1267_c0_g1	PEX4	Pollen-specific leucine-rich repeat extensin-like protein 4	−8.5	−5.05	−5.26	−8.04	−4.31	−3.62	
TRINITY_DN677_c0_g2	NPF8.2	Protein NRT1/PTR FAMILY 8,2	−2.24	−2.05	−2.36	−2.43			
TRINITY_DN7934_c0_g1	ABCG28	ABC transporter G family member 28	−2.78			−3.68	−4.42	7.31	
TRINITY_DN5923_c0_g1	OASA1	Cysteine synthase 1		2.1	2.13			9.71	
TRINITY_DN8399_c0_g1	RIC5	CRIB domain-containing protein RIC5					−4.82	−4.6	
TRINITY_DN8450_c0_g1	PPME1	Pectinesterase PPME1					−4.77		
TRINITY_DN5260_c2_g1	PEX1	Pollen-specific leucine-rich repeat extensin-like protein 1					−4.49	−3.64	
TRINITY_DN16608_c0_g2	RIC6	CRIB domain-containing protein RIC6					−4.2	−3.93	
TRINITY_DN184921_c0_g1	AGC1-5	Serine/threonine-protein kinase AGC1-5					−4.13		
TRINITY_DN35118_c0_g1	CNGC18	Cyclic nucleotide-gated ion channel 18					−3.97	6.14	
TRINITY_DN14636_c1_g1	CNGC7	Putative cyclic nucleotide-gated ion channel 7					−3.93	−4.53	
TRINITY_DN15772_c0_g3	CXE18	Probable carboxylesterase 18					−3.71		
TRINITY_DN8917_c0_g2	TOPP8	Serine/threonine-protein phosphatase PP1 isozyme 8					−3.98		
TRINITY_DN12354_c0_g2	KLCR2	Protein KINESIN LIGHT CHAIN-RELATED 2					−3.52	−3.57	
TRINITY_DN43059_c0_g1	TCTP1	Translationally-controlled tumor protein 1					−2.39	6.64	
TRINITY_DN145_c0_g1	AT2G41970	Probable protein kinase At2g41970					−2.03		
TRINITY_DN8899_c0_g3	ARAC11	Rac-like GTP-binding protein ARAC11					−2		
TRINITY_DN3041_c0_g3	CDI	Protein CDI						11.87	

Table 6. *Cont.*

Gene ID	Gene Name	Protein Name	M1a1	M1a2	M1o1	M1o2	M2a4	M2o4	M2d4
TRINITY_DN10453_c0_g1	AGC1-7	Serine/threonine-protein kinase AGC1-7						11.84	
TRINITY_DN7093_c0_g1	PIGA	Phosphatidylinositol N-acetylglucosaminyltransferase subunit A						10.57	
TRINITY_DN1136_c1_g1	FIM5	Fimbrin-5						10.5	
TRINITY_DN17922_c0_g2	WIP2	Zinc finger protein WIP2						−2.58	
TRINITY_DN6837_c0_g1	XI-C	Myosin-9						9.53	
TRINITY_DN9379_c0_g1	SBT3.1	Subtilisin-like protease SBT3.1						−2.11	
TRINITY_DN12065_c0_g1	MIRO1	Mitochondrial Rho GTPase 1						8.43	
pollen tube adhesion (GO:0009865)									
TRINITY_DN14184_c0_g1	HS1	Stress-response A/B barrel domain-containing protein HS1	−3.03			−2.2	−2.58	−2.22	
pollen-pistil interaction (GO:0009875)									
TRINITY_DN2016_c0_g1	MPK3	Mitogen-activated protein kinase 3	2.1				2.21	4.22	
TRINITY_DN4521_c0_g1	MAA3	Probable helicase MAGATAMA 3						12.13	
TRINITY_DN14556_c0_g1	MKK9	Mitogen-activated protein kinase kinase 9						9.61	
pollen maturation (GO:0010152)									
TRINITY_DN8479_c0_g1	DRP1C	Dynamin-related protein 1C						13.13	
TRINITY_DN13085_c0_g1	AFB2	Protein AUXIN SIGNALING F-BOX 2						9.73	
TRINITY_DN6009_c0_g1	RPK2	LRR receptor-like serine/threonine-protein kinase RPK2						3.81	
TRINITY_DN3540_c1_g1	PDR2	Probable manganese-transporting ATPase PDR2						2.12	
pollen tube guidance (GO:0010183)									
TRINITY_DN6442_c0_g1	A39	Aspartic proteinase 39	−2.79			−3.46	−3.7		
TRINITY_DN253_c1_g1	COBL10	COBRA-like protein 10	−8.86	−5.63	−5.6	−8.42	−4.18		
TRINITY_DN22116_c0_g1	MIK2	MDIS1-interacting receptor like kinase 2	2.62					8.29	−2.01
TRINITY_DN17193_c0_g1	MIK1	MDIS1-interacting receptor like kinase 1	−4.33			−3.54	−3.34	−4.58	
TRINITY_DN253_c0_g2	COBL11	COBRA-like protein 11					−4.68	−3.27	
TRINITY_DN30272_c0_g1	GEX3	Protein GAMETE EXPRESSED 3					−2.97		
TRINITY_DN20396_c0_g1	LIP2	Receptor-like kinase LIP2						9.71	
TRINITY_DN7012_c0_g1	SIZ1	E3 SUMO-protein ligase SIZ1						2.21	
TRINITY_DN5591_c0_g1	POD1	Protein POLLEN DEFECTIVE IN GUIDANCE 1						2.11	
pollen wall assembly (GO:0010208)									
TRINITY_DN6156_c0_g1	PKSA	Type III polyketide synthase A	−3.61		−6.78	−6.63	−3.39	−2.98	
TRINITY_DN17166_c0_g1	4CL3	4-coumarate–CoA ligase 3	−4.44		−2.69	−4.06	−3.78	−2.43	
TRINITY_DN923_c0_g1	CALS5	Callose synthase 5	−2.91		−2.05	−3.3	−3.49		
TRINITY_DN4588_c0_g2	ABCG31	ABC transporter G family member 31	−2.72	−3.81	−2.13	−2.53	−2.22	10.04	
TRINITY_DN45712_c0_g1	FAR2	Fatty acyl-CoA reductase 2. chloroplastic	−3.28		−6.24	−6.93	−4.07	−2.8	
TRINITY_DN9952_c0_g1	ABCG26	ABC transporter G family member 26					−3.28		
TRINITY_DN6869_c0_g1	A6	Probable glucan endo-1,3-β-glucosidase A6	−2.6		−7.57	−7.88	−2.61	−2.95	
TRINITY_DN31379_c0_g1	TKPR1	Tetraketide α-pyrone reductase 1					−4.21	−4.43	
TRINITY_DN156774_c0_g1	ABCG9	ABC transporter G family member 9					−2.19	−3.86	
TRINITY_DN3259_c0_g1	AHL16	AT-hook motif nuclear-localized protein 16	2.36	2.17		2.08	2.17		
TRINITY_DN6293_c0_g2	CYP703A2	Cytochrome P450 703A2						−3.11	
TRINITY_DN4485_c0_g1	CYP704B1	Cytochrome P450 704B1						−2.52	
pollen tube reception (GO:0010483)									
TRINITY_DN2319_c0_g2	FER	Receptor-like protein kinase FERONIA	−3.33	−2.02		−2.9	−2.85	−3.99	
TRINITY_DN1919_c0_g1	EVN	Dolichol kinase EVAN						3.02	
pollen exine formation (GO:0010584)									
TRINITY_DN6156_c0_g1	PKSA	Type III polyketide synthase A	−3.61		−6.78	−6.63	−3.39	−2.98	
TRINITY_DN17166_c0_g1	4CL3	4-coumarate–CoA ligase 3	−4.44		−2.69	−4.06	−3.78	−2.43	
TRINITY_DN45712_c0_g1	FAR2	Fatty acyl-CoA reductase 2. chloroplastic	−3.28		−6.24	−6.93	−4.07	−2.8	
TRINITY_DN6869_c0_g1	A6	Probable glucan endo-1,3-β-glucosidase A6	−2.6		−7.57	−7.88	−2.61	−2.95	
TRINITY_DN4186_c0_g1	QRT3	Polygalacturonase QRT3	−4.02	−3.09	−4.76	−4.77			
TRINITY_DN1609_c0_g1	BRI1	Protein BRASSINOSTEROID INSENSITIVE 1	−2.45				−2.2		
TRINITY_DN10341_c0_g1	PKSB	Type III polyketide synthase B			−2.2				
TRINITY_DN31379_c0_g1	TKPR1	Tetraketide α-pyrone reductase 1					−4.21	−4.43	
TRINITY_DN9952_c0_g1	ABCG26	ABC transporter G family member 26					−3.28		
TRINITY_DN6293_c0_g2	CYP703A2	Cytochrome P450 703A2						−3.11	
TRINITY_DN17210_c0_g1	IRX9H	Probable β-1,4-xylosyltransferase IRX9H						10.62	
TRINITY_DN8740_c0_g1	SHT	Spermidine hydroxycinnamoyl transferase						9.57	

Table 6. *Cont.*

Gene ID	Gene Name	Protein Name	M1a1	M1a2	M1o1	M1o2	M2a4	M2o4	M2d4
TRINITY_DN4485_c0_g1	CYP704B1	Cytochrome P450 704B1						−2.52	
TRINITY_DN42106_c0_g1	SSL13	Protein STRICTOSIDINE SYNTHASE-LIKE 13						8.48	
TRINITY_DN558_c0_g1	CDKG1	Cyclin-dependent kinase G1						3.14	
TRINITY_DN53293_c1_g1	TKPR2	Tetraketide α-pyrone reductase 2						6.87	
pollen sperm cell differentiation (GO:0048235)									
TRINITY_DN176325_c0_g1	COPT1	Copper transporter 1	−3.79	−3.86	−3.99	−3.76	−2.12		
TRINITY_DN16998_c0_g1	ZAT2	Zinc finger protein ZAT2					−4.9	−4.15	
TRINITY_DN31801_c4_g1	GPAT1	Glycerol-3-phosphate acyltransferase 1					−4.13	−4.38	
TRINITY_DN40616_c0_g1	QRT2	Polygalacturonase QRT2						6.55	−2.45
recognition of pollen (GO:0048544)									
TRINITY_DN10463_c0_g1	SD129	G-type lectin S-receptor-like serine/threonine-protein kinase SD1-29	3.45	3.42					
TRINITY_DN6512_c0_g1	SD16	Receptor-like serine/threonine-protein kinase SD1-6	2.13				2.14	2.61	
TRINITY_DN5252_c0_g2	AT5G24080	G-type lectin S-receptor-like serine/threonine-protein kinase At5g24080			2.26	−2.9			
TRINITY_DN38630_c0_g1	SD11	G-type lectin S-receptor-like serine/threonine-protein kinase SD1-1				−2.08		8.92	
TRINITY_DN2975_c0_g2	SD18	Receptor-like serine/threonine-protein kinase SD1-8						−3.11	
TRINITY_DN21172_c0_g1	RDR6	RNA-dependent RNA polymerase 6						−2.18	
TRINITY_DN10167_c0_g1	AT5G03700	PAN domain-containing protein At5g03700						−2.38	
TRINITY_DN151527_c0_g1	AT4G27290	G-type lectin S-receptor-like serine/threonine-protein kinase At4g27290						7.03	
microsporocyte nucleus (GO:0048556)									
TRINITY_DN42827_c0_g1	ARID1	AT-rich interactive domain-containing protein 1						10.37	
pollen tube development (GO:0048868)									
TRINITY_DN10227_c0_g2	CSLC12	Probable xyloglucan glycosyltransferase 12	−5.27	−3.31	−4.36	−5.35	−3.3		
TRINITY_DN2830_c0_g1	EDA30	Protein EMBRYO SAC DEVELOPMENT ARREST 30						11.59	
TRINITY_DN16425_c0_g1	LPPG	Lipid phosphate phosphatase γ						11.3	
TRINITY_DN1186_c1_g2	KCS5	3-ketoacyl-CoA synthase 5						−3.15	
TRINITY_DN65496_c0_g1	E1-β-2	Pyruvate dehydrogenase E1 component subunit β-3, chloroplastic						9.78	
TRINITY_DN14636_c1_g1	CNGC7	Putative cyclic nucleotide-gated ion channel 7					−3.93	−4.53	
TRINITY_DN8450_c0_g1	PPME1	Pectinesterase PPME1					−4.77		
TRINITY_DN691_c0_g2	ARAC5	Rac-like GTP-binding protein ARAC5	−3.62	−2.02	−2.9	−3.64	−2.65		
TRINITY_DN5487_c0_g1	ROPGEF12	Rop guanine nucleotide exchange factor 12					−5.33	−2.79	
TRINITY_DN923_c0_g1	CALS5	Callose synthase 5	−2.91		−2.05	−3.3	−3.49		
TRINITY_DN16608_c0_g2	RIC6	CRIB domain-containing protein RIC6					−4.2	−3.93	
TRINITY_DN145_c0_g1	AT2G41970	Probable protein kinase At2g41970					−2.03		
TRINITY_DN184921_c0_g1	AGC1-5	Serine/threonine-protein kinase AGC1-5					−4.13		
TRINITY_DN43059_c0_g1	TCTP1	Translationally-controlled tumor protein 1					−2.39	6.64	
TRINITY_DN1241_c0_g1	MGP4	UDP-D-xylose:L-fucose α-1,3-D-xylosyltransferase MGP4						2.88	
TRINITY_DN14184_c0_g1	HS1	Stress-response A/B barrel domain-containing protein HS1	−3.03			−2.2	−2.58	−2.22	
TRINITY_DN5260_c2_g1	PEX1	Pollen-specific leucine-rich repeat extensin-like protein 1					−4.49	−3.64	
TRINITY_DN8399_c0_g1	RIC5	CRIB domain-containing protein RIC5					−4.82	−4.6	
TRINITY_DN12354_c0_g2	KLCR2	Protein KINESIN LIGHT CHAIN-RELATED 2					−3.52	−3.57	
TRINITY_DN8899_c0_g3	ARAC11	Rac-like GTP-binding protein ARAC11					−2		
TRINITY_DN17193_c0_g1	MIK1	MDIS1-interacting receptor like kinase 1	−4.33			−3.54	−3.34	−4.58	
TRINITY_DN1267_c0_g1	PEX4	Pollen-specific leucine-rich repeat extensin-like protein 4	−8.5	−5.05	−5.26	−8.04	−4.31	−3.62	
TRINITY_DN35118_c0_g1	CNGC18	Cyclic nucleotide-gated ion channel 18					−3.97	6.14	

Table 6. *Cont.*

Gene ID	Gene Name	Protein Name	M1a1	M1a2	M1o1	M1o2	M2a4	M2o4	M2d4
TRINITY_DN30272_c0_g1	GEX3	Protein GAMETE EXPRESSED 3					−2.97		
TRINITY_DN15772_c0_g3	CXE18	Probable carboxylesterase 18					−3.71		
TRINITY_DN8917_c0_g2	TOPP8	Serine/threonine-protein phosphatase PP1 isozyme 8					−3.98		
microgametogenesis (GO:0055046)									
TRINITY_DN3449_c0_g1	PIRL3	Plant intracellular Ras-group-related LRR protein 3	2.7		2.74		3.21	2.39	
TRINITY_DN15578_c0_g1	LRL1	Transcription factor LRL1					−3.39	6.94	
TRINITY_DN4115_c0_g1	MYB35	Transcription factor MYB35						10.32	
TRINITY_DN593_c1_g2	KIN12A	Kinesin-like protein KIN-12A						8.1	
TRINITY_DN7491_c0_g1	AUG6	AUGMIN subunit 6						2.54	
rejection of self pollen (GO:0060320)									
TRINITY_DN124729_c0_g1	SPH5	S-protein homolog 5					−3.04		
acceptance of pollen (GO:0060321)									
TRINITY_DN12342_c0_g1	SEC5A	Exocyst complex component SEC5A						2.66	
pollen coat (GO:0070505)									
TRINITY_DN4588_c0_g2	ABCG31	ABC transporter G family member 31	−2.72	−3.81	−2.13	−2.53	−2.22	10.04	
TRINITY_DN156774_c0_g1	ABCG9	ABC transporter G family member 9					−2.19	−3.86	
regulation of pollen tube growth (GO:0080092)									
TRINITY_DN28088_c0_g2	RALFL19	Protein RALF-like 19	−7.67	−4.99	−4.97	−7.43	−4.92	−4.37	
TRINITY_DN6629_c0_g1	PRK4	Pollen receptor-like kinase 4	−6.87	−5.12	−4.56	−6.56	−4.64	−3.32	
TRINITY_DN5487_c0_g1	ROPGEF12	Rop guanine nucleotide exchange factor 12					−5.33	−2.79	
TRINITY_DN151480_c0_g1	CPK24	Calcium-dependent protein kinase 24					−4.88	−2.89	
TRINITY_DN8879_c0_g1	CPK17	Calcium-dependent protein kinase 17					−4.85	−2.86	
TRINITY_DN14172_c0_g1	PRK3	Pollen receptor-like kinase 3					−3.48	6.87	
TRINITY_DN9330_c2_g1	ROPGEF9	Rop guanine nucleotide exchange factor 9					−3.05		
TRINITY_DN6638_c1_g2	ROPGEF14	Rop guanine nucleotide exchange factor 14						−2.1	
TRINITY_DN37662_c0_g1	RABA4D	Ras-related protein RABA4d						7.85	
TRINITY_DN4047_c0_g1	AT1G60420	Probable nucleoredoxin 1						2.01	
TRINITY_DN3873_c0_g1	AGL65	Agamous-like MADS-box protein AGL65				−2.29	−2.62	−3.28	
TRINITY_DN12180_c0_g1	AGL66	Agamous-like MADS-box protein AGL66					−4.72	−3.81	
TRINITY_DN923_c0_g1	CALS5	Callose synthase 5	−2.91		−2.05	−3.3	−3.49		
TRINITY_DN1233_c4_g1	AT4G39110	Probable receptor-like protein kinase At4g39110	−8.01	−4.86	−4.65	−7.56	−4.44	−3.74	
pollen tube tip (GO:0090404)									
TRINITY_DN14105_c0_g1	ALA3	Phospholipid-transporting ATPase 3	2.51				3.12	10.21	
TRINITY_DN5561_c0_g1	ANX2	Receptor-like protein kinase ANXUR2	−7.96	−4.9	−5.05	−7.4	−4.33	−3.5	
pollen tube (GO:0090406)									
TRINITY_DN41664_c0_g1	ZAR1	Receptor protein kinase-like protein ZAR1	−2.54	−2.17	−2.01	−2.43			
TRINITY_DN6369_c0_g1	PLT1	Putative polyol transporter 1	−2.03		−2.04				
TRINITY_DN29983_c0_g1	AT4G36180	Probable LRR receptor-like serine/threonine-protein kinase At4g36180	−3.9		−2.83	−4.51			
TRINITY_DN6280_c0_g1	STP8	Sugar transport protein 8	−4.78	−2.96	−4.96	−4.45		10.23	
TRINITY_DN4295_c0_g1	INT2	Probable inositol transporter 2			2.38			2.79	
TRINITY_DN15838_c0_g1	TIP5-1	Probable aquaporin TIP5-1				−2.48	−2.82	8.26	
TRINITY_DN12736_c0_g1	LLG2	GPI-anchored protein LLG2					−4.35	−2.64	
TRINITY_DN165958_c0_g1	GATL4	Probable galacturonosyltransferase-like 4					−4.18	−4.06	
TRINITY_DN11246_c1_g1	GNL2	ARF guanine-nucleotide exchange factor GNL2					−2.8	−2.87	
TRINITY_DN63597_c0_g1	MDIS2	Protein MALE DISCOVERER 2					−2.26	9.33	
TRINITY_DN9084_c0_g1	SUC3	Sucrose transport protein SUC3						11.54	
TRINITY_DN18602_c0_g1	SAUR62	Auxin-responsive protein SAUR62						9.11	
TRINITY_DN38341_c0_g1	STP7	Sugar transport protein 7						2.55	

4. Discussion

An increasing number of molecular studies have identified several candidate genes implicated in the shift from sexual to apomixis reproduction [18,21,22,70]. In different species, apomixis has been found to arise due to the action or deregulation of different genes associated with the normal sexual pathway [23,71–73]. Nevertheless, it is still not fully understood how these genes alter reproductive pathways to establish apomixis.

In most apomictic wild species. Implementing omics approaches can be particularly challenging as complete genomic sequences are not available and, therefore, genome annotation information is not available. Additionally, obtaining plant material for transcriptomic studies can be an experimentally challenging task in *Limonium* since each plant presents a single ovary, enclosed in a calyx and inner, medium, and outer bracts that yield just a single basal ovule [13]. In the current study, we performed a comparative transcriptome analysis between sexual and asexual plants and identified candidate genes that are specifically or differentially expressed between reproductive modes and among stages of ovule development. This approach allowed us to disclose differential regulation of both HKGs as well as genes specifically involved in flower development, male sterility, and pollen recognition, besides major pathways potentially central to apomixis, including protein degradation, transcription, stress response, hormonal signaling, signal transduction, and epigenetic regulation.

4.1. Differential Regulation of HKG and Metabolic Pathways in Sexual and Apomictic Plants

In this study, the total number of expressed unigenes among samples was higher in ovules from apomictic plants than in those from sexual plants, together with a differential regulation of genes, particularly in the later stages of ovule development (Table 1). Previous studies between sexual and asexual plants provided support for the deregulation of reproductive pathways, including HKGs in, e.g., *Boechera holboellii* complex [72], *Brachiaria* [74], *Cenchrus ciliaris* [75], and *Ranunculus* [73], among others. In this study, although many homolog genes in *Arabidopsis* were stably expressed in *Limonium*, such as *ACT* domain-containing proteins. Cytosolic Fe-S cluster assembly factors *NBP35*, NADH dehydrogenase [ubiquinone] flavoprotein 2, phosphoglycerate kinase 1, polyubiquitin 3, TATA-box binding protein 2, and other HKGs were found to be differentially expressed. These include genes related to the ubiquitin degradation process, such as ubiquitin-conjugating enzymes, tubulin, actin, and elongation factor-1 α as found in other sexual and apomictic plants' complexes above referred. Therefore, some of the HKGs identified (Table 3) in our study can be potentially used as reference genes to be validated in future quantitative gene expression studies using different developmental stages of specific tissue types or different reproductive modes.

A differential representation of DEGs in *Limonium* sexual and apomictic plants associated with the oxidative stress response was found. In apomictic plants, some of these DEGs (Supplementary Figure S5), e.g., *ACO3*, *CDSP32*, *GSH1*, etc., were up-regulated while others were down-regulated (*GR1*, *GASA14*, and *GSTF11*) in both the initial (apomeiosis) and later (parthenogenesis) stages of ovule development. Nonetheless, apomicts present more up-regulated DEGs regarding oxidative stress than sexual plants, supporting the involvement of redox reactions in this reproductive mode. Alteration of homeostasis-based processes of stress perception and attenuation in sexual species of several genera would induce apomeiotic spores and gametophyte formation [23]. Apomeiosis occurs when the redox balance is more toward H_2O_2 catabolism, and the transition from meiosis to apomeiosis can be changed by a disturbance in this homeostasis [23].

Among DEGs between sexual and *Limonium* apomicts, most were up-regulated in the latter stages of ovule development (parthenogenesis), such as *ATRX* genes coding for chromatin remodelling proteins as well as multiple histone methylation genes concerning epigenetic developmental mechanisms in plants [76] (Tables 5 and 6). These DEGs were also previously found to be upregulated, for instance, in parthenogenetic eggs of *Cenchrus ciliaris* [77]. Moreover, other DEGs implicated in small RNA biogenesis and DNA-methylation pathways, such as the *AGO9* and *AGO4* homolog genes in *Arabidopsis* mutants found to be associated with phenotypes reminiscent of apospory or diplospory [78], were also detected in our study. In *Boechera* apomicts, *AGO9* was found at low levels in the megaspore mother cell itself, becoming an apomictic initial cell [79]. However, in our study, *AGO4* and *AGO9* seem to have more specific roles in ovules at later stages of development (parthenogenesis), likely being involved in eggs assuming a parthenogenesis fate. MAPK

signaling and aminoacyl-tRNA biosynthesis pathways that perform roles in translational regulation, RNA splicing, and tRNA proofreading [80] also showed transcriptional changes at this stage in apomictic *Limonium* plants (Tables 5 and 6).

DEGs were also remarkably enriched in genes implicated in hormonal signaling, such as the ethylene signaling pathway, in which the apomictic gametophytes overexpressed 26 ethylene-responsive transcription factors (Tables 5 and 6). For example, in *Cenchrus ciliaris*, EIN2 (ethylene insensitive 2) together with 14 ethylene responsive transcription factors were up-regulated in parthenogenetic eggs [77], although in our study both genes showed contrasting expression patterns in the same developmental stage (parthenogenesis). Moreover, in the parthenogenetic ovules, overexpressed genes were related to tryptophan metabolism, such as *TAA1* (l-tryptophan pyruvate aminotransferase), which converts tryptophan to indole-pyruvic acid, a direct biosynthetic precursor of the auxin in *Arabidopsis* (IAA [81]). Crosstalk between ethylene signaling and auxin pathways is involved in the regulation of developmental processes [82].

4.2. Feminization of Apomicts Is Related to Down-Regulation of Floral Genes Specifying Stamens

Besides auxin, other hormones like gibberellic acid (GA) contribute to flower development, the development of male and female gametophytes, and seed germination [83.84]. The GASA genes as well as the GA biosynthesis genes in *Arabidopsis*, implicated in controlling floral induction, seed maturation, and germination [83,84], were differentially expressed between apomictic and sexual plants in our study (Table 4). One of the targets of GA signaling are the floral homeotic genes encoding MADS-box transcription factors involved in floral development in accordance with the ABCDE model [85]. In our study, among the top DEGs between sexual and apomictic plants and between the different ovule stages, MADS-box transcription factors were identified, including floral homeotic genes with a MADS-box domain. In *A. thaliana*, the MADS-box from A-class genes (*AP1*; *AP2*) specifies the formation of sepals; the combination of A- and B-class genes (*AP3*; *PI*) determines petal' development; the B-, C- (*AGL*), and E-class (*SEP*) genes specify stamens; and the C- and E-class genes specify carpels. Only the expression of genes from class C specifies carpel formation. Class E genes (*SEP3*) are associated with the formation of all flower whorls. The gene classes A and C are expressed antagonistically; the A gene class is expressed in sepals and petals, and the C gene class is expressed in stamens and carpels [86,87].

GA promotes reproductive development by upregulating expression of the floral meristem identity gene LEAFY (*LFY*), which in turn upregulates expression of *AP3* and *AGL* that, in conjunction with *PI* and *SEP3*, regulate floral organ identity [87]. In our study, we found changes in the expression of MADS-box genes in the different stages of ovule development between sexual and apomictic plants, particularly *PI*, *SEP1*, and *AP3* genes, which were downregulated in apomicts. The *PI/AP3* genes have a role in sexual dimorphism and have been identified as masculinizing factors in spinach [88]. In dioecious plants such as *Populus*, constitutive overexpression of *PI/AP3* produces male flowers, but in female flowers the presence of a feminizing factor F downregulates *PI/AP3*, diverting development to a female developmental pathway, inhibiting stamens, and allowing carpels to form [89]. Therefore, it could be hypothesized that male sterile *Limonium* plants with homeotic changes in floral organs lack the gene function of the corresponding class B genes.

4.3. Male Sterility Appears to Be Linked with Downregulation of Genes Connected to Pollen Wall Formation and Assembly and Pollen Tube Growth

Various genes are involved in pollen wall development and assembly, which is a specialized extracellular cell wall matrix that encases the male gametophytes [90]. A specific cell wall polymer also known as β-glucan is synthesized by callose synthases in pollen mother cells and microspore tetrads that acts as a template for primexine, thus providing a structural basis for exine formation [90]. Callose synthase 5 (*CSL5*) is a key isoform of callose synthases responsible for the formation of the callose wall, which is essential for the

accumulation of callose in the tube wall and the callose plug in growing pollen tubes [91]. In *CSL5* mutants, the viability of pollen grains is greatly reduced in *Arabidopsis* [91,92] and rice [93]. In our study in *Limonium, CSL5* is downregulated in the initial (apomeiosis) and later phases of development (parthenogenesis) in the apomicts. One of the characteristic features of plants in the *L. binervosum* group is the widespread existence of male sterility, i.e., a lack of pollen [12,13,26,36]. Electron microscopy studies showed that *L. multiflorum* plants had many flowers with empty anthers and sometimes flowers with no pollen at all; the few microspores that formed showed collapsed morphology and lacked the typical exine patterns [12]. In *L. multiflorum* apomicts, after anther dehiscence releases pollen, the plants never undergo their first mitosis, only attaining the "ring vacuolate" stage, and the male germ unit is not produced [12]. Interestingly, in this study, callose synthase isoforms such as *CSL9* or *CSL11* that were upregulated in the apomicts have a role in *Arabidopsis* pollen mitosis by disrupting pollen mitosis and producing pollen with only one or two nuclei, the generative cell being degenerated, undifferentiated, or mislocalized [94,95], as found here in *Limonium*.

Moreover, in our study, the gene *PEX4* that codes for extracellular glycoproteins that belong to the hydroxyproline-rich glycoprotein family and have a role in pollen germination and pollen tube growth in *A. thaliana* [96,97]. was downregulated in *Limonium* apomicts (apomeiosis, M1a1). The *PEX4* mutants have an excessive deposition of callose [96,97], leading to abnormal pollen tubes that develop bulges and burst [97]. While in *L. multiflorum* apomicts, pollen tubes are never observed since unicellular pollen never undergoes its first mitosis. In *L. ovalifolium* sexual plants, pollen grains follow a first asymmetric mitotic division, producing a generative cell within the vegetative pollen grain cell in the binucleate pollen stage [12]. Therefore, our results support a role for *PEX4* in pollen tube growth. Perhaps this gene, along with other unknown genes, might create a terminal combination that does not allow the development of pollen tubes.

4.4. Pollen-Stigma Interactions

Pollen-pistil interactions can be viewed as a major prezygotic pollination reproductive barrier and are active systems of pollen rejection [98]. Some of these systems act at the level of the stigma, with a genetic control independent from embryo sac development involving S-alleles [99]. In the Brassicaceae family, the SI is controlled sporophytically by a single S locus that incorporates stigma-expressed and anther-expressed genes composed of multiple alleles or variants [100]. In various gametophytic apomicts, non-functional pollen can cause a weakening of SI and a breakdown of the sporophytic SI system (mentor effects [9]).

Limonium species show a polymorphic sexual system associated with flower polymorphisms and a sporophytic self-incompatibility that prevents self- and intramorph mating [29.30]. *Limonium* gametophytic apomicts that form diplosporic (apomictic) embryo sacs of *Rudbeckia* type like in *L. multiflorum* [13] show abnormal and non-functional pollen due to a sporophytic defect [12]. In our study, in the GO term "recognition of pollen" (GO:0048544; Table 6). All DEGs were lectin receptor kinases (LECRKs) [101], except for AT3G49500. These kinases belong to the class of G-LECRKs [101], particularly the S-locus Receptor Kinase (SRK), known for its role in self-incompatibility [101] and potentially of high interest in our studied species. In our study, DEGs from this LECRKs complex were detected under the GO term "recognition of pollen", namely AT1G61380, AT1G65800, AT5G24080, AT4G27300, AT4G21380, and AT4G27290. Four DEGs of the SRK were overexpressed, namely in the initial stages of ovule development (apomeiosis), such as AT1G61380 (M1a1 and M1a2) and AT1G65800 (M1a1), as well as in later ovule stages (M2a4 and M2o4), AT4G27300 (M2o4), and AT4G27290 (M2o4). These findings indicate that the genes implicated in pollen recognition in *Limonium* were already expressed at earlier ovule stages. This implies that the fate of the gametophytic apomict male spores is decided by the maternal genes in the initial ovule stages. Nonetheless, a genetic linkage between SI and apomixis cannot be easily assumed, since the breakdown of SI mostly affects the pollen and the stigma, while apomixis affects the development of the embryo sac.

4.5. Up-Regulation of Specific Genes Related with Embryo Formation in the Apomicts

In *Arabidopsis,* flowering can be promoted by repressing the transcription of the central flowering repressor and vernalization regulatory gene *FLC* (FLOWERING LOCUS C), which belongs to the MADS-box class of transcription factors [102]. The *FLC* seems to regulate several transcription factors involved in important biological processes such as reproductive and embryonic development [103]. *FLC* impedes the floral transition by inhibiting the expression of the floral primordium identity genes such as *FT* (FLOWERING LOCUS T), *SOC1/AGL20* (SUPPRESSOR OF CONSTANS OVEREXPRESSION 1/AG20), *LFY*, *AP1*, and floral organ identity *AG* and *AP3* genes [104]. Another gene involved in the genetic control of flowering time in *Arabidopsis* is *FPF1* (FLOWERING PROMOTING FACTOR), which modulates the acquisition of competence to flower in the apical meristem and is expressed earlier than *AP1* [105]. In our study, the *FPF1* and *SOC1* showed higher levels of regulation in apomicts than in sexual plants, whereas *AP1* showed reduced levels in the first ones. These results indicate differences in the regulation of major genes controlling the transition from a vegetative to a reproductive mode in the apomict's apical meristem. Interestingly, in our study, both *FLC*, *AGL6*, and *AGL15*, as well as other MADS-box transcription factors, were specifically upregulated in the later stages of development. In *A. thaliana AGL6* functions in the early stages of the flowering signal transduction pathway by inhibiting the transcription of *FLC* genes [106]. In *Brachiaria brizantha*, *AGL6* is differentially expressed during embryo sac formation in apomictic and sexual plants [107]. In our study, *AGL15*, which plays an essential role during early zygotic embryogenesis in *Arabidopsis* [108], in *Brassica napus,* and in soyabean somatic embryos [109], was specifically upregulated in the later phase of ovule development in *Limonium* apomicts. The *AGL15* is a component of the SERK protein complex [110] that is part of a molecular network linked to zygotic and somatic embryogenesis. However, in this study, we were unable to find any differential expression of SERK-like genes.

Some genes related to the bioactive gibberellins' deactivation reaction from the GA2OX family were differentially expressed. For example, *GA2OX6* was up-regulated in both the initial and later stages of ovule development. While in *A. thaliana*, *GA2OX6* expression is activated by *AGL15* during embryogenesis [111], in our study, *AGL15* was down-regulated in M2a4 and up-regulated in M2o4, suggesting differences among species. Moreover, *GA2OX6* is found to be expressed in sepals, stigmas, and immature anthers. Regarding seed development, it was only expressed in the antipodal cells before the 8-cell stage, suggesting that this gene is a negative regulator of seed germination [111]. Remarkably, from the same family, *GA2OX8*, which is exclusively expressed in stomatal cells in *A. thaliana* but is not expressed or has distinct expression patterns in flower tissues or seed development [111], was down-regulated in *Limonium* apomicts in later stages of ovule development (parthenogenesis). This finding supports the idea that this gene can have other or different roles in *Limonium*.

5. Conclusions

This study sheds light on genes involved in *Limonium* sexual and apomictic reproduction. The findings substantiate the deregulation of gene expression in the regular sexual pathway. While several HKGs are found to be differentially expressed between sexual and asexual plants, other genes are found to be stably expressed. These can be potentially used as reference genes to be validated for specific tissue types (vegetative and reproductive) or reproductive modes (sexual and apomictic) in future quantitative gene expression studies. Our findings reveal that the latter stage of ovule development (parthenogenesis) was the most contrasting phase in terms of differential gene expression between asexual and sexual plants. Among them, the MADS-box domain TFs are central players in many developmental processes, including control of flowering time, homeotic regulation of floral organogenesis, fruit development, and seed pigmentation.

Since *L. multiflorum* male sterile plants form parthenogenetic ovule sacs, it could be interesting to analyze candidate genes such as *PEX4* in pollen tube development and

the function of AGL genes (e.g., *AGL6*) specifically modulated in the latter stages of development (parthenogenesis). Nonetheless, given the high number of 71% unannotated genes in *Limonium*, other studies are required to clarify the regulatory roles of these genes.

References

1. Hojsgaard, D.; Greilhuber, J.; Pellino, M.; Paun, O.; Sharbel, T.F.; Hörandl, E. Emergence of apospory and bypass of meiosis via apomixis after sexual hybridisation and polyploidisation. *New Phytol.* **2014**, *204*, 1000–1012. [CrossRef]
2. Asker, S.E.; Jerling, L. *Apomixis in Plants*, 1st ed.; CRC Press: Boca Raton, FL, USA, 1992.
3. Richards, A.J. *Plant Breeding Systems*; Chapman and Hall: London, UK, 1997.
4. Koltunow, A.M.; Grossniklaus, U. Apomixis: A developmental perspective. *Annu. Rev. Plant Biol.* **2003**, *54*, 547–574. [CrossRef]
5. Talent, N.; Dickinson, T.A. Endosperm formation in apposporous Crataegus. Rosaceae, Spiraeoideae, tribe Pyreae): Parallels to Ranunculaceae and Poaceae. *New Phytol.* **2007**, *173*, 231–249. [CrossRef] [PubMed]

6.   Nogler, G.A. Gametophytic apomixis. In *Embryology of Angiosperms, Johri, B.M., Ed.*; Springer-Verlag: Berlin, Germany, 1984; pp. 475–518.

7.   Naumova, T.N.; Mershchikova, I. *Apomixis in Angiosperms: Nucellar and Integumentary Embryony*; CRC Press: Boca Raton, FL, USA, 2018.

8.   Whitton, J.; Sears, C.J.; Baack, E.; Otto, S.P. The dynamic nature of apomixis in the angiosperms. *Int. J. Plant Sci.* **2008**, *169*, 169–182. [CrossRef]

9.   Tas, I.C.; Van Dijk, P.J. Crosses between sexual and apomictic dandelions (Taraxacum). I. The inheritance of apomixis. *Heredity* **1999**, *83*, 707–714. [CrossRef]

10.   Meirmans, P.G.; Den Nijs, J.C.; Van Tienderen, P.H. Male sterility in triploid dandelions: Asexual females vs. asexual hermaphrodites. *Heredity* **2006**, *96*, 45–52. [CrossRef]

11.   Thompson, S.L.; Choe, G.; Ritland, K.; Whitton, J. Cryptic sex within male-sterile polyploid populations of the easter daisy, Townsendia hookeri. *Int. J. Plant Sci.* **2008**, *169*, 183–193. [CrossRef]

12.   Róis, A.S.; Teixeira, G.; Sharbel, T.F.; Fuchs, J.; Martins, S.; Espírito-Santo, D.; Caperta, A.D. Male fertility versus sterility, cytotype, and DNA quantitative variation in seed production in diploid and tetraploid sea lavenders (Limonium sp., Plumbaginaceae) reveal diversity in reproduction modes. *Sex Plant Reprod.* **2012**, *25*, 305–318. [CrossRef]

13.   Róis, A.S.; Sádio, F.; Paulo, O.S.; Teixeira, G.; Paes, A.P.; Espírito-Santo, D.; Caperta, A.D. Phylogeography and modes of reproduction in diploid and tetraploid halophytes of Limonium species (Plumbaginaceae): Evidence for a pattern of geographical parthenogenesis. *Ann. Bot.* **2016**, *117*, 37–50. [CrossRef] [PubMed]

14.   Caetano, A.P.S.; Cortez, P.A.; Teixeira, S.P.; Oliveira, P.E.; Carmello-Guerreiro, S.M. Unusual diversity of apomictic mechanisms in a species of Miconia, Melastomataceae. *Plant Syst. Evol.* **2018**, *304*, 343–355. [CrossRef]

15.   Nygren, A. The genesis of some Scandinavian species of Calamagrostis. *Hereditas* **1946**, *32*, 131–262. [CrossRef] [PubMed]

16.   Czapik, R. Problems of apomictic reproduction in the families Compositae and Rosaceae. *Folia Geobot.* **1996**, *31*, 381–387. [CrossRef]

17.   Barcaccia, G.; Albertini, E. Apomixis in plant reproduction: A novel perspective on an old dilemma. *Plant Reprod.* **2013**, *26*, 159–179. [CrossRef] [PubMed]

18.   Hand, M.L.; Koltunow, A.M. The genetic control of apomixis: Asexual seed formation. *Genetics* **2014**, *197*, 441–450. [CrossRef]

19.   Carman, J.G. Asynchronous expression of duplicate genes in angiosperms may cause apomixis, bispory, tetraspory, and polyembryony. *Biol. J. Linn. Soc.* **1997**, *61*, 51–94. [CrossRef]

20.   León-Martínez, G.; Vielle-Calzada, J.P. Apomixis in flowering plants: Developmental and evolutionary considerations. *Curr. Top. Dev.* **2019**, *131*, 565–604. [CrossRef]

21.   Schmidt, A. Controlling apomixis: Shared features and distinct characteristics of gene regulation. *Genes* **2020**, *11*, 329. [CrossRef]

22.   Brukhin, V. Molecular and genetic regulation of apomixis. *Russ. J. Genet.* **2017**, *53*, 943–964. [CrossRef]

23.   Mateo de Arias, M.; Gao, L.; Sherwood, D.A.; Dwivedi, K.K.; Price, B.J.; Jamison, M.; Kowalis, B.M.; Carman, J.G. Whether gametophytes are reduced or unreduced in angiosperms might be determined metabolically. *Genes* **2020**, *11*, 1449. [CrossRef]

24.   Conceição, S.I.R.; Róis, A.S.; Caperta, A.D. Limonium homoploid and heteroploid intra- and interspecific crosses unveil seed anomalies and neopolyploidy related to sexual and/or apomictic reproduction. *Taxon* **2018**, *67*, 1153–1162. [CrossRef]

25.   Erben, M. Die gattung Limonium im südwestmediterranen Raum. *Mitt. Bot. Staatssamml. Münch.* **1978**, *14*, 361–626.

26.   Ingrouille, M.J.; Stace, C.A. Pattern of variation of agamospermous Limonium (Plumbaginaceae) in the British Isles. *Nordic J. Bot.* **1985**, *5*, 113–125. [CrossRef]

27.   Cowan, R.; Ingrouille, M.J.; Lledó, M.D. The taxonomic treatment of agamosperms in the genus Limonium Mill. (Plumbaginaceae). *Folia Geobot.* **1998**, *33*, 353–366. [CrossRef]

28.   Caperta, A.D.; Conceição, S.I.; Róis, A.S.; Loureiro, J.; Castro, S. Cytogenetic features of sexual and asexual Limonium taxa (Plumbaginaceae). *Taxon* **2018**, *67*, 1143–1152. [CrossRef]

29.   Baker, H.G. Dimorphism and monomorphism in the Plumbaginaceae: II. Pollen and stigmata in the genus Limonium. *Ann. Bot.* **1953**, *17*, 433–446. [CrossRef]

30.   Baker, H.G. The evolution, functioning and breakdown of heteromorphic incompatibility systems. I. The Plumbaginaceae. *Evolution* **1966**, *20*, 349–368. [CrossRef] [PubMed]

31.   Conceição, S.I.R.; Fernandes, J.; Borges da Silva, E.; Caperta, A.D. Reproductive output and insect behavior in hybrids and apomicts from Limonium ovalifolium and L. binervosum complexes (Plumbaginaceae) in an open cross-pollination experiment. *Plants* **2021**, *10*, 169. [CrossRef] [PubMed]

32.   D'Amato, F. Contributo all'embriologia delle Plumbaginaceae. *Nuov. Giorn. Bot. Ital.* **1940**, *47*, 349–382. [CrossRef]

33.   D'Amato, F. Triploidia e apomissia in Statice oleaefolia Scop. var. confusa Godr. *Caryologia* **1949**, *2*, 71–84. [CrossRef]

34.   Hjelmqvist, H.; Grazi, E. Studies on variation in embryo sac development. *Bot. Not.* **1964**, *118*, 329–360.

35.   Conceição, S.I.R.; Róis, A.S.; Caperta, A.D. Nonreduction via meiotic restitution and pollen heterogeneity may explain residual male fertility in triploid marine halophyte Limonium algarvense (Plumbaginaceae). *Caryologia* **2019**, *72*, 53–62. [CrossRef]

36.   Ingrouille, M.J.; Stace, C.A. The Limonium binervosum aggregate (Plumbaginaceae) in the British Isles. *Bot. J. Linn. Soc.* **1986**, *92*, 177–217. [CrossRef]

37.   Del Guacchio, E.; Erben, M.; Caputo, P. The neglected name Statice auriculifolia (Plumbaginaceae) and its related names: A long history of nomenclatural intricacy. *Taxon* **2019**, *68*, 1093–1100. [CrossRef]

38. Soneson, C.; Delorenzi, M.A. Comparison of methods for differential expression analysis of RNA-seq data. *BMC Bioinform.* **2013**, *14*, 91. [CrossRef]

39. Morgan, E.R.; Burge, G.K.; Seelye, J.F.; Hopping, M.E.; Grant, J.E. Production of inter-specific hybrids between Limonium perezii (Stapf) Hubb. and *Limonium sinuatum* (L.) Mill. *Euphytica* **1998**, *102*, 109–115. [CrossRef]

40. Andrews, S. FastQC: A Quality Control Tool for High Throughput Sequence Data. 2010. Available online: http://www.bioinformatics.babraham.ac.uk/projects/fastqc (accessed on 8 September 2020).

41. Wingett, S.W.; Andrews, S. FastQ Screen: A tool for multi-genome mapping and quality control. *F1000Research* **2018**, *7*, 1338. [CrossRef] [PubMed]

42. Bolger, A.M.; Lohse, M.; Usadel, B. Trimmomatic: A flexible trimmer for Illumina sequence data. *Bioinformatics* **2014**, *30*, 2114–2120. [CrossRef]

43. Grabherr, M.G.; Haas, B.J.; Yassour, M.; Levin, J.Z.; Thompson, D.A.; Amit, I.; Adiconis, X.; Fan, L.; Raychowdhury, R.; Zeng, Q.; et al. Full-length transcriptome assembly from RNA-seq data without a reference genome. *Nat. Biotechnol.* **2011**, *29*, 644–652. [CrossRef]

44. Wang, S.; Gribskov, M. Comprehensive evaluation of de novo transcriptome assembly programs and their effects on differential gene expression analysis. *Bioinformatics* **2016**, *33*, 327–333. [CrossRef]

45. Waterhouse, R.M.; Seppey, M.; Simão, F.A.; Manni, M.; Ioannidis, P.; Klioutchnikov, G.; Kriventseva, E.V.; Zdobnov, E.M. BUSCO applications from quality assessments to gene prediction and phylogenomics. *Mol. Biol. Evol.* **2018**, *31*, 3210–3212. [CrossRef]

46. Nishimura, O.; Hara, Y.; Kuraku, S. gVolante for standardizing completeness assessment of genome and transcriptome assemblies. *Bioinformatics* **2017**, *33*, 3635–3637. [CrossRef] [PubMed]

47. Langmead, B.; Salzberg, S.L. Fast gapped-read alignment with Bowtie 2. *Nat. Methods* **2012**, *9*, 357–359. [CrossRef] [PubMed]

48. Li, B.; Dewey, C.N. RSEM: Accurate transcript quantification from RNA-Seq data with or without a reference genome. *BMC Bioinform.* **2011**, *12*, 323. [CrossRef] [PubMed]

49. R Core Team. *R: A Language and Environment for Statistical Computing*; R Foundation for Statistical Computing: Vienna, Austria, 2010. Available online: https://www.R-project.org/ (accessed on 7 September 2020).

50. Robinson, M.D.; McCarthy, D.J.; Smyth, G.K. edgeR: A Bioconductor package for differential expression analysis of digital gene expression data. *Bioinformatics* **2010**, *26*, 139–140. [CrossRef]

51. Chen, Y.; Lun, A.T.L.; Smyth, G.K. Differential expression analysis of complex RNA-seq experiments using edgeR. In *Statistical Analysis of Next Generation Sequencing Data. Frontiers in Probability and the Statistical Sciences*; Datta, S., Nettleton, D., Eds.; Springer: Cham, Switzerland, 2014; pp. 51–74. [CrossRef]

52. Caswell, T.A.; Droettboom, M.; Lee, A.; Hunter, J.H.; Sales de Andrade, E.; Hoffman, T.; Stansby, D.; Klymak, J.; Varoquaux, N.; Hedegaard, N.J.; et al. matplotlib/matplotlib: REL: v3.3.3 (Version v3.3.3). *Zenodo* **2020**. [CrossRef]

53. Chen, C.; Huang, H.; Wu, C.H. Protein Bioinformatics Databases and Resources. *Methods Mol. Biol.* **2017**, *1558*, 3–39. [CrossRef]

54. Van Ex, F.; Jacob, Y.; Martienssen, R.A. Multiple roles for small RNAs during plant reproduction. *Curr. Opin. Plant Biol.* **2011**, *14*, 588–593. [CrossRef]

55. Petrella, R.; Cucinotta, M.; Mendes, M.A.; Underwood, C.J.; Colombo, L. The emerging role of small RNAs in ovule development, a kind of magic. *Plant Reprod.* **2021**, *34*, 335–351. [CrossRef]

56. Zinta, G.; Khan, A.; Abd Elgawad, H.; Verma, V.; Srivastava, A.K. Unveiling the redox control of plant reproductive development during abiotic stress. *Front. Plant Sci.* **2016**, *7*, 700. [CrossRef]

57. Sundberg, E.; Østergaard, L. Distinct and dynamic auxin activities during reproductive development. *Cold Spring Harb. Perspect. Biol.* **2009**, *1*, a001628. [CrossRef]

58. Larsson, E.; Vivian-Smith, A.; Offringa, R.; Sundberg, E. Auxin homeostasis in Arabidopsis ovules is anther-dependent at maturation and changes dynamically upon fertilization. *Front. Plant Sci.* **2017**, *8*, 1735. [CrossRef] [PubMed]

59. Dambacher, S.; Hahn, M.; Schotta, G. Epigenetic regulation of development by histone lysine methylation. *Heredity* **2010**, *105*, 24–37. [CrossRef]

60. Rose, N.R.; Klose, R.J. Understanding the relationship between DNA methylation and histone lysine methylation. *BBA* **2014**, *1839*, 1362–1372. [CrossRef] [PubMed]

61. Arora, R.; Agarwal, P.; Ray, S.; Singh, A.K.; Singh, V.P.; Tyagi, A.K.; Kapoor, S. MADS-box gene family in rice: Genome-wide identification, organization and expression profiling during reproductive development and stress. *BMC Genom.* **2007**, *8*, 242. [CrossRef]

62. Castelán-Muñoz, N.; Herrera, J.; Cajero-Sánchez, W.; Arrizubieta, M.; Trejo, C.; García-Ponce, B.; de la Sánchez, M.P.; Álvarez-Buylla, E.R.; Garay-Arroyo, A. MADS-Box genes are key components of genetic regulatory networks involved in abiotic stress and plastic developmental responses in plants. *Front. Plant Sci.* **2019**, *10*, 853. [CrossRef]

63. Shah, L.; Sohail, A.; Ahmad, R.; Cheng, S.; Cao, L.; Wu, W. The roles of MADS-Box genes from root growth to maturity in Arabidopsis and rice. *Agronomy* **2022**, *12*, 582. [CrossRef]

64. Figueroa, P.; Browse, J. Male sterility in Arabidopsis induced by overexpression of a MYC5-SRDX chimeric repressor. *Plant J.* **2015**, *81*, 849–860. [CrossRef] [PubMed]

65. Khouider, S.; Borges, F.; LeBlanc, C.; Ungru, A.; Schnittger, A.; Martienssen, R.; Colot, V.; Bouyer, D. Male fertility in Arabidopsis requires active DNA demethylation of genes that control pollen tube function. *Nat. Commun.* **2021**, *12*, 410. [CrossRef] [PubMed]

66. Zheng, Y.; Jiao, C.; Sun, H.; Rosli, H.G.; Pombo, M.A.; Zhang, P.; Banf, M.; Dai, X.; Martin, G.B.; Giovannoni, J.J.; et al. iTAK: A program for genome-wide prediction and classification of plant transcription factors, transcriptional regulators, and protein kinases. *Mol. Plant* **2016**, *9*, 1667–1670. [CrossRef]

67. Raudvere, U.; Kolberg, L.; Kuzmin, I.; Arak, T.; Adler, P.; Peterson, H.; Vilo, J.G. Profiler: A web server for functional enrichment analysis and conversions of gene lists. *Nucleic Acids Res.* **2019**, *47*, W191–W198. [CrossRef]

68. Supek, F.; Bošnjak, M.; Škunca, N.; Šmuc, T. REVIGO summarizes and visualizes long lists of Gene Ontology terms. *PLoS ONE* **2011**, *6*, e21800. [CrossRef] [PubMed]

69. Wickham, H. *ggplot2: Elegant Graphics for Data Analysis*; Springer-Verlag: New York, NY, USA, 2016.

70. Pupilli, F.; Barcaccia, G. Cloning plants by seeds: Inheritance models and candidate genes to increase fundamental knowledge for engineering apomixis in sexual crops. *J. Biotechnol.* **2012**, *159*, 291–311. [CrossRef] [PubMed]

71. Polegri, L.; Calderini, O.; Arcioni, S.; Pupilli, F. Specific expression of apomixis-linked alleles revealed by comparative transcriptomic analysis of sexual and apomictic Paspalum simplex Morong flowers. *JXB* **2010**, *61*, 1869–1883. [CrossRef] [PubMed]

72. Sharbel, T.F.; Voigt, M.L.; Corral, J.M.; Galla, G.; Kumlehn, J.; Klukas, C.; Schreiber, F.; Vogel, H.; Rotter, B. Apomictic and sexual ovules of Boechera display heterochronic global gene expression patterns. *Plant Cell* **2010**, *22*, 655–671. [CrossRef]

73. Pellino, M.; Hojsgaard, D.; Hörandl, E.; Sharbel, T.F. Chasing the apomictic factors in the Ranunculus auricomus complex: Exploring gene expression patterns in microdissected sexual and apomictic ovules. *Genes* **2020**, *11*, 728. [CrossRef]

74. Silveira, E.D.; Alves-Ferreira, M.; Guimarães, L.A.; Silva, F.R.; Carneiro, V.T.C. Selection of reference genes for quantitative real-time PCR expression studies in the apomictic and sexual grass Brachiaria brizantha. *BMC Plant Biol.* **2009**, *9*, 84. [CrossRef]

75. Simon, B.; Conner, J.A.; Ozias-Akins, P. Selection and validation of reference genes for gene expression analysis in apomictic and sexual Cenchrus ciliaris. *BMC Res. Notes* **2013**, *6*, 397. [CrossRef]

76. Duc, C.; Benoit, M.; Détourné, G.; Simon, L.; Poulet, A.; Jung, M.; Veluchamy, A.; Latrasse, D.; Le Goff, S.; Cotterell, S.; et al. Arabidopsis ATRX modulates H3.3 occupancy and fine-tunes gene expression. *Plant Cell* **2017**, *29*, 1773–1793. [CrossRef]

77. Ke, Y.; Podio, M.; Conner, J.; Ozias-Akins, P. Single-cell transcriptome profiling of buffelgrass (*Cenchrus ciliaris*) eggs unveils apomictic parthenogenesis signatures. *Sci. Rep.* **2021**, *11*, 9880. [CrossRef]

78. Olmedo-Monfil, V.; Durán-Figueroa, N.; Arteaga-Vázquez, M.; Demesa-Arévalo, E.; Autran, D.; Grimanelli, D.; Slotkin, R.K.; Martienssen, R.A.; Vielle-Calzada, J.-P. Control of female gamete formation by a small RNA pathway in Arabidopsis. *Nature* **2010**, *464*, 628–632. [CrossRef]

79. Schmidt, A.; Schmid, M.W.; Klostermeier, U.C.; Qi, W.; Guthörl, D.; Sailer, C.; Waller, M.; Rosenstiel, P.; Grossniklaus, U. Apomictic and sexual germline development differ with respect to cell cycle, transcriptional, hormonal and epigenetic regulation. *PLoS Genet.* **2014**, *10*, e1004476. [CrossRef]

80. Berg, M.; Rogers, R.; Muralla, R.; Meinke, D. Requirement of aminoacyl-tRNA synthetases for gametogenesis and embryo development in Arabidopsis. *Plant J.* **2005**, *44*, 866–878. [CrossRef]

81. Zhao, Y. Auxin biosynthesis and its role in plant development. *Ann. Rev. Plant Biol.* **2010**, *61*, 49–64. [CrossRef]

82. Zemlyanskaya, E.V.; Omelyanchuk, N.A.; Ubogoeva, E.V.; Mironova, V.V. Deciphering auxin-ethylene crosstalk at a systems level. *Int. J. Mol. Sci.* **2018**, *19*, 4060. [CrossRef]

83. Finch-Savage, W.E.; Leubner-Metzger, G. Seed dormancy and the control of germination. *New Phytol.* **2006**, *171*, 501–523. [CrossRef]

84. Plackett, A.R.; Thomas, S.G.; Wilson, Z.A.; Hedden, P. Gibberellin control of stamen development: A fertile field. *Trends Plant Sci.* **2011**, *16*, 568–578. [CrossRef]

85. Liu, Z.; Mara, C. Regulatory mechanisms for floral homeotic gene expression. *Semin. Cell Dev. Biol.* **2010**, *21*, 80–86. [CrossRef]

86. Coen, E.S.; Meyerowitz, E.M. The war of the whorls: Genetic interactions controlling flower development. *Nature* **1991**, *353*, 31–37. [CrossRef]

87. Airoldi, C.A. Determination of sexual organ development. *Sex. Plant Reprod.* **2010**, *23*, 53–62. [CrossRef]

88. Sather, D.N.; Jovanovic, M.; Golenberg, E.M. Functional analysis of B and C class floral organ genes in spinach demonstrates their role in sexual dimorphism. *BMC Plant Biol.* **2010**, *10*, 46. [CrossRef]

89. Cronk, Q.; Müller, N.A. Default sex and single gene sex determination in dioecious plants. *Front. Plant Sci.* **2020**, *11*, 1162. [CrossRef]

90. Shi, J.; Cui, M.; Yang, L.; Kim, Y.-J.; Zhang, D. Genetic and biochemical mechanisms of pollen wall development. *Trends Plant Sci.* **2015**, *20*, 741–753. [CrossRef]

91. Dong, X.; Hong, Z.; Sivaramakrishnan, M.; Mahfouz, M.; Verma, D.P.S. Callose synthase (CalS5) is required for exine formation during microgametogenesis and for pollen viability in Arabidopsis. *Plant J.* **2005**, *42*, 315–328. [CrossRef]

92. Nishikawa, S.; Zinkl, G.M.; Swanson, R.J.; Maruyama, D.; Preuss, D. Callose (beta-1,3 glucan) is essential for Arabidopsis pollen wall patterning, but not tube growth. *BMC Plant Biol.* **2005**, *5*, 22. [CrossRef]

93. Shi, X.; Sun, X.; Zhang, Z.; Han, L.; Wu, J.; Lu, T. GLUCAN SYNTHASE-LIKE 5 (GSL5) plays an essential role in male fertility by regulating callose metabolism during microsporogenesis in rice. *Plant Cell Physiol.* **2015**, *56*, 497–509. [CrossRef]

94. Töller, A.; Brownfield, L.; Neu, C.; Twell, D.; Schulze-Lefert, P. Dual function of Arabidopsis glucan synthase-like genes GSL8 and GSL10 in male gametophyte development and plant growth. *Plant J.* **2008**, *54*, 911–923. [CrossRef]

95. Huang, L.; Chen, X.Y.; Rim, Y.; Han, X.; Cho, W.K.; Kim, S.-W.; Kim, J.-Y. Arabidopsis glucan synthase-like 10 functions in male gametogenesis. *J. Plant Physiol.* **2009**, *166*, 344–352. [CrossRef]

96. Fabrice, T.N.; Vogler, H.; Draeger, C.; Munglani, G.; Gupta, S.; Herger, A.G.; Knox, P.; Grossniklaus, U.; Ringli, C. LRX proteins play a crucial role in pollen grain and pollen tube cell wall development. *Plant Physiol.* **2018**, *176*, 1981–1992. [CrossRef]

97. Sede, A.R.; Borassi, C.; Wengier, D.L.; Mecchia, M.A.; Estevez, J.M.; Muschietti, J.P. Arabidopsis pollen extensins LRX are required for cell wall integrity during pollen tube growth. *FEBS Lett.* **2018**, *592*, 233–243. [CrossRef]

98. Charlesworth, D.; Vekemans, X.; Castric, V.; Glémin, S. Plant self-incompatibility systems: A molecular evolutionary perspective. *New Phytol.* **2005**, *168*, 61–69. [CrossRef]

99. de Nettancourt, D. The basic features of self-Incompatibility. In *Incompatibility and Incongruity in Wild and Cultivated Plants*, 2nd ed.; Springer: Berlin, Germany, 2001; pp. 1–24. [CrossRef]

100. Kusaba, M.; Dwyer, K.; Hendershot, J.; Vrebalov, J.; Nasrallah, J.B.; Nasrallah, M.E. Self-incompatibility in the genus Arabidopsis: Characterization of the S locus in the outcrossing A. lyrata and its autogamous relative A. thaliana. *Plant Cell* **2001**, *13*, 627–643. [CrossRef]

101. Teixeira, M.A.; Rajewski, A.; He, J.; Castaneda, O.G.; Litt, A.; Kaloshian, I. Classification and phylogenetic analyses of the Arabidopsis and tomato G-type lectin receptor kinases. *BMC Genom.* **2018**, *19*, 239. [CrossRef]

102. Cheng, Z.; Ge, W.; Li, L.; Hou, D.; Ma, Y.; Liu, J.; Bai, Q.; Li, X.; Mu, S.; Gao, J. Analysis of MADS-Box gene family reveals conservation in floral organ ABCDE model of Moso bamboo (Phyllostachys edulis). *Front. Plant Sci.* **2017**, 656. [CrossRef]

103. Deng, W.; Ying, H.; Helliwell, C.A.; Taylor, J.M.; Peacock, W.J.; Denis, E.S. FLOWERING LOCUS C (FLC) regulates development pathways throughout the life cycle of Arabidopsis. *PNAS* **2011**, *108*, 6680–6685. [CrossRef]

104. Kobayashi, Y.; Weigel, D. Move on up, it's time for change–Mobile signals controlling photoperiod-dependent flowering. *Genes Dev.* **2007**, *21*, 2371–2384. [CrossRef]

105. Melzer, S.; Kampmann, G.; Chandler, J.; Apel, K. FPF1 modulates the competence to flowering in Arabidopsis. *Plant J.* **1999**, *18*, 395–405. [CrossRef]

106. Koo, S.C.; Bracko, O.; Park, M.S.; Schawb, R.; Chun, H.J.; Park, K.M.; Seo, J.S.; Grbic, V.; Balasubramanian, S.; Schmid, M.; et al. Control of lateral organ development and flowering time by the Arabidopsis thaliana MADS-box Gene AGAMOUS-LIKE6. *Plant J.* **2010**, *62*, 807–816. [CrossRef]

107. Guimarães, L.A.; de Dusi, D.M.A.; Masiero, S.; Resentini, F.; Gomes, A.C.M.M.; Silveira, E.D.; Florentino, L.H.; Rodrigues, J.C.M.; Colombo, L.; Carneiro, V.T. BbrizAGL6 Is differentially expressed during embryo sac formation of apomictic and sexual Brachiaria brizantha plants. *Plant Mol. Biol. Rep.* **2013**, *31*, 1397–1406. [CrossRef]

108. Perry, S.E.; Lehti, M.D.; Fernandez, D.E. The MADS-domain protein AGAMOUS-like 15 accumulates in embryonic tissues with diverse origins. *Plant Physiol.* **1999**, *120*, 121–130. [CrossRef]

109. Thakare, D.; Tang, W.; Hill, K.; Perry, S.E. The MADS-domain transcriptional regulator AGAMOUS-LIKE15 promotes somatic embryo development in Arabidopsis and soybean. *Plant Physiol.* **2008**, *146*, 1663–1672. [CrossRef]

110. Karlova, R.; Boeren, S.; Russinova, E.; de Vries, S. The Arabidopsis SOMATIC EMBRYOGENESIS RECEPTOR-LIKE KINASE1 protein complex includes Brassinosteroid-Insensitive1. *Plant Cell* **2006**, *18*, 626–638. [CrossRef]

111. Li, B.; Chen, X.; Wu, Y.; Gu, A.; Zhang, J.; Luo, S.; Gao, X.; Zhao, J.; Pan, X.; Shen, S. Gene characterization and molecular pathway analysis of reverse thermosensitive genic male sterility in eggplant (*Solanum melongena* L.). *Hortic. Res.* **2019**, *6*, 118. [CrossRef]